5

MCMC Using Hamiltonian Dynamics

Radford M. Neal

5.1 Introduction

Markov chain Monte Carlo (MCMC) originated with the classic paper of Metropolis et al. (1953), where it was used to simulate the distribution of states for a system of idealized molecules. Not long after, another approach to molecular simulation was introduced (Alder and Wainwright, 1959), in which the motion of the molecules was deterministic, following Newton's laws of motion, which have an elegant formalization as *Hamiltonian dynamics*. For finding the properties of bulk materials, these approaches are asymptotically equivalent, since even in a deterministic simulation, each local region of the material experiences effectively random influences from distant regions. Despite the large overlap in their application areas, the MCMC and molecular dynamics approaches have continued to coexist in the following decades (see Frenkel and Smit, 1996).

In 1987, a landmark paper by Duane, Kennedy, Pendleton, and Roweth united the MCMC and molecular dynamics approaches. They called their method "hybrid Monte Carlo," which abbreviates to "HMC," but the phrase "Hamiltonian Monte Carlo," retaining the abbreviation, is more specific and descriptive, and I will use it here. Duane et al. applied HMC not to molecular simulation, but to lattice field theory simulations of quantum chromodynamics. Statistical applications of HMC began with my use of it for neural network models (Neal, 1996a). I also provided a statistically-oriented tutorial on HMC in a review of MCMC methods (Neal, 1993, Chapter 5). There have been other applications of HMC to statistical problems (e.g. Ishwaran, 1999; Schmidt, 2009) and statistically-oriented reviews (e.g. Liu, 2001, Chapter 9), but HMC still seems to be underappreciated by statisticians, and perhaps also by physicists outside the lattice field theory community.

This review begins by describing Hamiltonian dynamics. Despite terminology that may be unfamiliar outside physics, the features of Hamiltonian dynamics that are needed for HMC are elementary. The differential equations of Hamiltonian dynamics must be discretized for computer implementation. The "leapfrog" scheme that is typically used is quite simple.

Following this introduction to Hamiltonian dynamics, I describe how to use it to construct an MCMC method. The first step is to define a Hamiltonian function in terms of the probability distribution we wish to sample from. In addition to the variables we are interested in (the "position" variables), we must introduce auxiliary "momentum" variables, which typically have independent Gaussian distributions. The HMC method alternates simple updates for these momentum variables with Metropolis updates in which a new state is proposed by computing a trajectory according to Hamiltonian dynamics, implemented with the leapfrog method. A state proposed in this way can be distant from the

current state but nevertheless have a high probability of acceptance. This bypasses the slow exploration of the state space that occurs when Metropolis updates are done using a simple random-walk proposal distribution. (An alternative way of avoiding random walks is to use short trajectories but only partially replace the momentum variables between trajectories, so that successive trajectories tend to move in the same direction.)

After presenting the basic HMC method, I discuss practical issues of tuning the leapfrog stepsize and number of leapfrog steps, as well as theoretical results on the scaling of HMC with dimensionality. I then present a number of variations on HMC. The acceptance rate for HMC can be increased for many problems by looking at "windows" of states at the beginning and end of the trajectory. For many statistical problems, approximate computation of trajectories (e.g. using subsets of the data) may be beneficial. Tuning of HMC can be made easier using a "short-cut" in which trajectories computed with a bad choice of stepsize take little computation time. Finally, "tempering" methods may be useful when multiple isolated modes exist.

5.2 Hamiltonian Dynamics

Hamiltonian dynamics has a physical interpretation that can provide useful intuitions. In two dimensions, we can visualize the dynamics as that of a frictionless puck that slides over a surface of varying height. The state of this system consists of the *position* of the puck, given by a two-dimensional vector q, and the *momentum* of the puck (its mass times its velocity), given by a two-dimensional vector p. The *potential energy*, $U(q)$, of the puck is proportional to the height of the surface at its current position, and its *kinetic energy*, $K(p)$, is equal to $|p|^2/(2m)$, where m is the mass of the puck. On a level part of the surface, the puck moves at a constant velocity, equal to p/m. If it encounters a rising slope, the puck's momentum allows it to continue, with its kinetic energy decreasing and its potential energy increasing, until the kinetic energy (and hence p) is zero, at which point it will slide back down (with kinetic energy increasing and potential energy decreasing).

In nonphysical MCMC applications of Hamiltonian dynamics, the position will correspond to the variables of interest. The potential energy will be minus the log of the probability density for these variables. Momentum variables, one for each position variable, will be introduced artificially.

These interpretations may help motivate the exposition below, but if you find otherwise, the dynamics can also be understood as simply resulting from a certain set of differential equations.

5.2.1 Hamilton's Equations

Hamiltonian dynamics operates on a d-dimensional *position* vector, q, and a d-dimensional *momentum* vector, p, so that the full state space has $2d$ dimensions. The system is described by a function of q and p known as the *Hamiltonian*, $H(q, p)$.

5.2.1.1 Equations of Motion

The partial derivatives of the Hamiltonian determine how q and p change over time, t, according to Hamilton's equations:

$$\frac{dq_i}{dt} = \frac{\partial H}{\partial p_i}, \tag{5.1}$$

$$\frac{dp_i}{dt} = -\frac{\partial H}{\partial q_i}, \tag{5.2}$$

for $i = 1, \ldots, d$. For any time interval of duration s, these equations define a mapping, T_s, from the state at any time t to the state at time $t + s$. (Here, H, and hence T_s, are assumed to not depend on t.)

Alternatively, we can combine the vectors q and p into the vector $z = (q, p)$ with $2d$ dimensions, and write Hamilton's equations as

$$\frac{dz}{dt} = J\,\nabla H(z),$$

where ∇H is the gradient of H (i.e. $[\nabla H]_k = \partial H/\partial z_k$), and

$$J = \begin{bmatrix} 0_{d\times d} & I_{d\times d} \\ -I_{d\times d} & 0_{d\times d} \end{bmatrix} \tag{5.3}$$

is a $2d \times 2d$ matrix whose quadrants are defined above in terms of identity and zero matrices.

5.2.1.2 Potential and Kinetic Energy

For HMC we usually use Hamiltonian functions that can be written as

$$H(q, p) = U(q) + K(p). \tag{5.4}$$

Here $U(q)$ is called the *potential energy*, and will be defined to be minus the log probability density of the distribution for q that we wish to sample, plus any constant that is convenient. $K(p)$ is called the *kinetic energy*, and is usually defined as

$$K(p) = p^T M^{-1} p/2. \tag{5.5}$$

Here M is a symmetric, positive-definite "mass matrix," which is typically diagonal, and is often a scalar multiple of the identity matrix. This form for $K(p)$ corresponds to minus the log probability density (plus a constant) of the zero-mean Gaussian distribution with covariance matrix M.

With these forms for H and K, Hamilton's equations 5.1 and 5.2 can be written as follows, for $i = 1, \ldots, d$:

$$\frac{dq_i}{dt} = [M^{-1}p]_i, \tag{5.6}$$

$$\frac{dp_i}{dt} = -\frac{\partial U}{\partial q_i}. \tag{5.7}$$

5.2.1.3 A One-Dimensional Example

Consider a simple example in one dimension (for which q and p are scalars and will be written without subscripts), in which the Hamiltonian is defined as follows:

$$H(q,p) = U(q) + K(p), \qquad U(q) = \frac{q^2}{2}, \quad K(p) = \frac{p^2}{2}. \tag{5.8}$$

As we will see later in Section 5.3.1, this corresponds to a Gaussian distribution for q with mean zero and variance one. The dynamics resulting from this Hamiltonian (following Equations 5.6 and 5.7) is

$$\frac{dq}{dt} = p, \quad \frac{dp}{dt} = -q.$$

Solutions have the following form, for some constants r and a:

$$q(t) = r\cos(a+t), \quad p(t) = -r\sin(a+t). \tag{5.9}$$

Hence, the mapping T_s is a rotation by s radians clockwise around the origin in the (q,p) plane. In higher dimensions, Hamiltonian dynamics generally does not have such a simple periodic form, but this example does illustrate some important properties that we will look at next.

5.2.2 Properties of Hamiltonian Dynamics

Several properties of Hamiltonian dynamics are crucial to its use in constructing MCMC updates.

5.2.2.1 Reversibility

First, Hamiltonian dynamics is *reversible*—the mapping T_s from the state at time t, $(q(t), p(t))$, to the state at time $t+s$, $(q(t+s), p(t+s))$, is one-to-one, and hence has an inverse, T_{-s}. This inverse mapping is obtained by simply negating the time derivatives in Equations 5.1 and 5.2. When the Hamiltonian has the form in Equation 5.4, and $K(p) = K(-p)$, as in the quadratic form for the kinetic energy of Equation 5.5, the inverse mapping can also be obtained by negating p, applying T_s, and then negating p again.

In the simple one-dimensional example of Equation 5.8, T_{-s} is just a counterclockwise rotation by s radians, undoing the clockwise rotation of T_s.

The reversibility of Hamiltonian dynamics is important for showing that MCMC updates that use the dynamics leave the desired distribution invariant, since this is most easily proved by showing reversibility of the Markov chain transitions, which requires reversibility of the dynamics used to propose a state.

5.2.2.2 Conservation of the Hamiltonian

A second property of the dynamics is that it *keeps the Hamiltonian invariant* (i.e. conserved). This is easily seen from Equations 5.1 and 5.2 as follows:

$$\frac{dH}{dt} = \sum_{i=1}^{d}\left[\frac{dq_i}{dt}\frac{\partial H}{\partial q_i} + \frac{dp_i}{dt}\frac{\partial H}{\partial p_i}\right] = \sum_{i=1}^{d}\left[\frac{\partial H}{\partial p_i}\frac{\partial H}{\partial q_i} - \frac{\partial H}{\partial q_i}\frac{\partial H}{\partial p_i}\right] = 0. \tag{5.10}$$

With the Hamiltonian of Equation 5.8, the value of the Hamiltonian is half the squared distance from the origin, and the solutions (Equation 5.9) stay at a constant distance from the origin, keeping H constant.

For Metropolis updates using a proposal found by Hamiltonian dynamics, which form part of the HMC method, the acceptance probability is one if H is kept invariant. We will see later, however, that in practice we can only make H approximately invariant, and hence we will not quite be able to achieve this.

5.2.2.3 Volume Preservation

A third fundamental property of Hamiltonian dynamics is that it *preserves volume* in (q, p) space (a result known as Liouville's theorem). If we apply the mapping T_s to the points in some region R of (q, p) space, with volume V, the image of R under T_s will also have volume V.

With the Hamiltonian of Equation 5.8, the solutions (Equation 5.9) are rotations, which obviously do not change the volume. Such rotations also do not change the shape of a region, but this is not so in general—Hamiltonian dynamics might stretch a region in one direction, as long as the region is squashed in some other direction so as to preserve volume.

The significance of volume preservation for MCMC is that we need not account for any change in volume in the acceptance probability for Metropolis updates. If we proposed new states using some arbitrary, non-Hamiltonian, dynamics, we would need to compute the determinant of the Jacobian matrix for the mapping the dynamics defines, which might well be infeasible.

The preservation of volume by Hamiltonian dynamics can be proved in several ways. One is to note that the divergence of the vector field defined by Equations 5.1 and 5.2 is zero, which can be seen as follows:

$$\sum_{i=1}^{d} \left[\frac{\partial}{\partial q_i} \frac{dq_i}{dt} + \frac{\partial}{\partial p_i} \frac{dp_i}{dt} \right] = \sum_{i=1}^{d} \left[\frac{\partial}{\partial q_i} \frac{\partial H}{\partial p_i} - \frac{\partial}{\partial p_i} \frac{\partial H}{\partial q_i} \right] = \sum_{i=1}^{d} \left[\frac{\partial^2 H}{\partial q_i \partial p_i} - \frac{\partial^2 H}{\partial p_i \partial q_i} \right] = 0.$$

A vector field with zero divergence can be shown to preserve volume (Arnold, 1989).

Here, I will show informally that Hamiltonian dynamics preserves volume more directly, without presuming this property of the divergence. I will, however, take as given that volume preservation is equivalent to the determinant of the Jacobian matrix of T_s having absolute value one, which is related to the well-known role of this determinant in regard to the effect of transformations on definite integrals and on probability density functions.

The $2d \times 2d$ Jacobian matrix of T_s, seen as a mapping of $z = (q, p)$, will be written as B_s. In general, B_s will depend on the values of q and p before the mapping. When B_s is diagonal, it is easy to see that the absolute values of its diagonal elements are the factors by which T_s stretches or compresses a region in each dimension, so that the product of these factors, which is equal to the absolute value of $\det(B_s)$, is the factor by which the volume of the region changes. I will not prove the general result here, but note that if we were to (say) rotate the coordinate system used, B_s would no longer be diagonal, but the determinant of B_s is invariant to such transformations, and so would still give the factor by which the volume changes.

Let us first consider volume preservation for Hamiltonian dynamics in one dimension (i.e. with $d = 1$), for which we can drop the subscripts on p and q. We can approximate T_δ

for δ near zero as follows:

$$T_\delta(q,p) = \begin{bmatrix} q \\ p \end{bmatrix} + \delta \begin{bmatrix} dq/dt \\ dp/dt \end{bmatrix} + \text{terms of order } \delta^2 \text{ or higher.}$$

Taking the time derivatives from Equations 5.1 and 5.2, the Jacobian matrix can be written as

$$B_\delta = \begin{bmatrix} 1 + \delta \dfrac{\partial^2 H}{\partial q \partial p} & \delta \dfrac{\partial^2 H}{\partial p^2} \\ -\delta \dfrac{\partial^2 H}{\partial q^2} & 1 - \delta \dfrac{\partial^2 H}{\partial p \partial q} \end{bmatrix} + \text{terms of order } \delta^2 \text{ or higher.} \tag{5.11}$$

We can then write the determinant of this matrix as

$$\begin{aligned} \det(B_\delta) &= 1 + \delta \frac{\partial^2 H}{\partial q \partial p} - \delta \frac{\partial^2 H}{\partial p \partial q} + \text{terms of order } \delta^2 \text{ or higher} \\ &= 1 + \text{terms of order } \delta^2 \text{ or higher.} \end{aligned}$$

Since $\log(1+x) \approx x$ for x near zero, $\log\det(B_\delta)$ is zero, except perhaps for terms of order δ^2 or higher (though we will see later that it is exactly zero). Now consider $\log\det(B_s)$ for some time interval s that is not close to zero. Setting $\delta = s/n$, for some integer n, we can write T_s as the composition of T_δ applied n times (from n points along the trajectory), so $\det(B_s)$ is the n-fold product of $\det(B_\delta)$ evaluated at these points. We then find that

$$\begin{aligned} \log\det(B_s) &= \sum_{i=1}^{n} \log\det(B_\delta) \\ &= \sum_{i=1}^{n} \Big\{ \text{terms of order } 1/n^2 \text{ or smaller} \Big\} \\ &= \text{terms of order } 1/n \text{ or smaller.} \end{aligned} \tag{5.12}$$

Note that the value of B_δ in the sum in Equation 5.12 might perhaps vary with i, since the values of q and p vary along the trajectory that produces T_s. However, assuming that trajectories are not singular, the variation in B_δ must be bounded along any particular trajectory. Taking the limit as $n \to \infty$, we conclude that $\log\det(B_s) = 0$, so $\det(B_s) = 1$, and hence T_s preserves volume.

When $d > 1$, the same argument applies. The Jacobian matrix will now have the following form (compare Equation 5.11), where each entry shown below is a $d \times d$ submatrix, with rows indexed by i and columns by j:

$$B_\delta = \begin{bmatrix} I + \delta \left[\dfrac{\partial^2 H}{\partial q_j \partial p_i} \right] & \delta \left[\dfrac{\partial^2 H}{\partial p_j \partial p_i} \right] \\ -\delta \left[\dfrac{\partial^2 H}{\partial q_j \partial q_i} \right] & I - \delta \left[\dfrac{\partial^2 H}{\partial p_j \partial q_i} \right] \end{bmatrix} + \text{terms of order } \delta^2 \text{ or higher.}$$

As for $d = 1$, the determinant of this matrix will be one plus terms of order δ^2 or higher, since all the terms of order δ cancel. The remainder of the argument above then applies without change.

5.2.2.4 Symplecticness

Volume preservation is also a consequence of Hamiltonian dynamics being *symplectic*. Letting $z = (q, p)$, and defining J as in Equation 5.3, the symplecticness condition is that the Jacobian matrix, B_s, of the mapping T_s satisfies

$$B_s^T J^{-1} B_s = J^{-1}.$$

This implies volume conservation, since $\det(B_s^T)\det(J^{-1})\det(B_s) = \det(J^{-1})$ implies that $\det(B_s)^2$ is one. When $d > 1$, the symplecticness condition is stronger than volume preservation. Hamiltonian dynamics and the symplecticness condition can be generalized to where J is any matrix for which $J^T = -J$ and $\det(J) \neq 0$.

Crucially, reversibility, preservation of volume, and symplecticness can be maintained exactly even when, as is necessary in practice, Hamiltonian dynamics is approximated, as we will see next.

5.2.3 Discretizing Hamilton's Equations—The Leapfrog Method

For computer implementation, Hamilton's equations must be approximated by discretizing time, using some small stepsize, ε. Starting with the state at time zero, we iteratively compute (approximately) the state at times $\varepsilon, 2\varepsilon, 3\varepsilon$, etc.

In discussing how to do this, I will assume that the Hamiltonian has the form $H(q, p) = U(q) + K(p)$, as in Equation 5.4. Although the methods below can be applied with any form for the kinetic energy, I assume for simplicity that $K(p) = p^T M^{-1} p/2$, as in Equation 5.5, and furthermore that M is diagonal, with diagonal elements $m_1, \ldots, m_d$, so that

$$K(p) = \sum_{i=1}^{d} \frac{p_i^2}{2m_i}. \tag{5.13}$$

5.2.3.1 Euler's Method

Perhaps the best-known way to approximate the solution to a system of differential equations is Euler's method. For Hamilton's equations, this method performs the following steps, for each component of position and momentum, indexed by $i = 1, \ldots, d$:

$$p_i(t + \varepsilon) = p_i(t) + \varepsilon \frac{dp_i}{dt}(t) = p_i(t) - \varepsilon \frac{\partial U}{\partial q_i}(q(t)), \tag{5.14}$$

$$q_i(t + \varepsilon) = q_i(t) + \varepsilon \frac{dq_i}{dt}(t) = q_i(t) + \varepsilon \frac{p_i(t)}{m_i}. \tag{5.15}$$

The time derivatives in Equations 5.14 and 5.15 are from the form of Hamilton's equations given by Equations 5.6 and 5.7. If we start at $t = 0$ with given values for $q_i(0)$ and $p_i(0)$, we can iterate the steps above to get a trajectory of position and momentum values

at times $\varepsilon, 2\varepsilon, 3\varepsilon, \ldots$, and hence find (approximate) values for $q(\tau)$ and $p(\tau)$ after τ/ε steps (assuming τ/ε is an integer).

Figure 5.1a shows the result of using Euler's method to approximate the dynamics defined by the Hamiltonian of Equation 5.8, starting from $q(0) = 0$ and $p(0) = 1$, and using a stepsize of $\varepsilon = 0.3$ for 20 steps (i.e. to $\tau = 0.3 \times 20 = 6$). The results are not good—Euler's method produces a trajectory that diverges to infinity, but the true trajectory is a circle. Using a smaller value of ε, and correspondingly more steps, produces a more accurate result at $\tau = 6$, but although the divergence to infinity is slower, it is not eliminated.

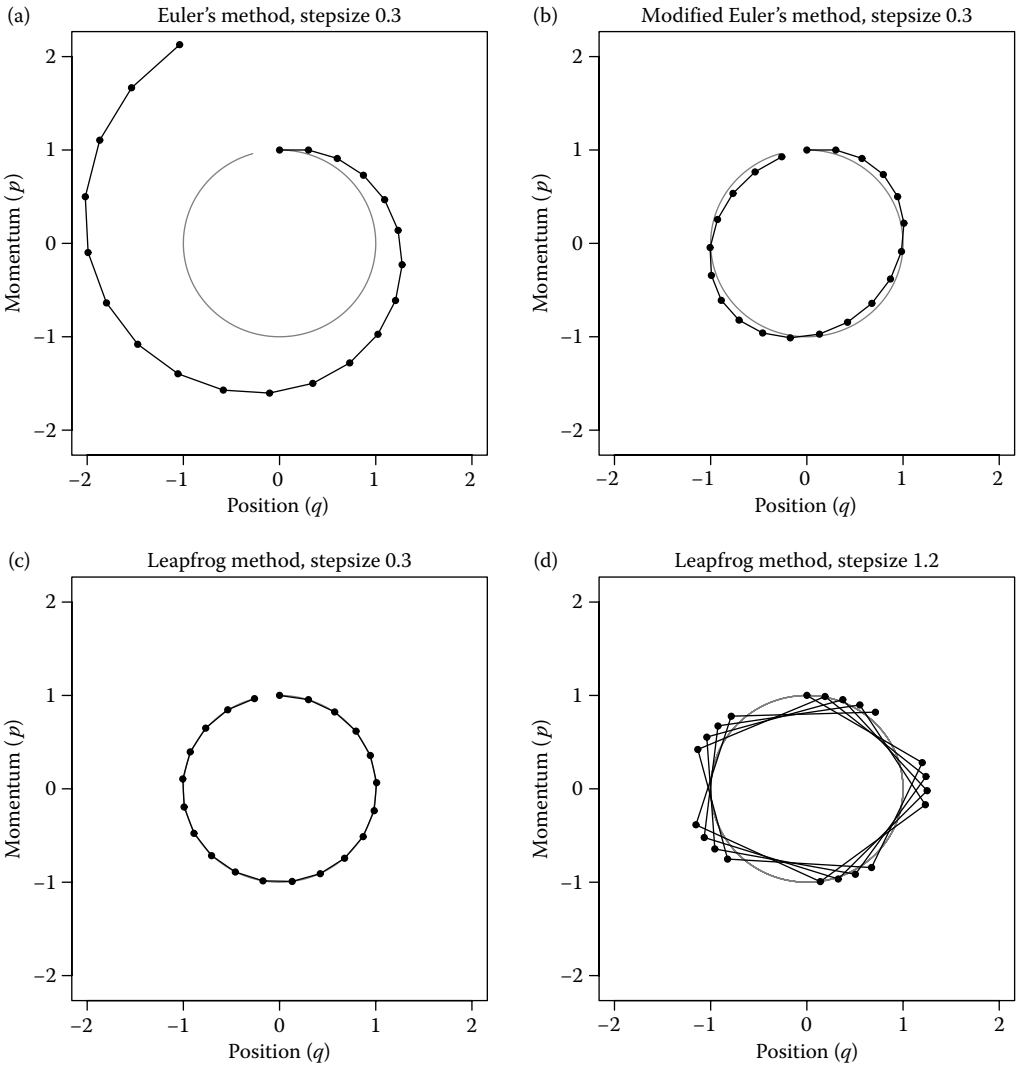

FIGURE 5.1
Results using three methods for approximating Hamiltonian dynamics, when $H(q, p) = q^2/2 + p^2/2$. The initial state was $q = 0, p = 1$. The stepsize was $\varepsilon = 0.3$ for (a), (b), and (c), and $\varepsilon = 1.2$ for (d). Twenty steps of the simulated trajectory are shown for each method, along with the true trajectory (in gray).

5.2.3.2 A Modification of Euler's Method

Much better results can be obtained by slightly modifying Euler's method, as follows:

$$p_i(t + \varepsilon) = p_i(t) - \varepsilon \frac{\partial U}{\partial q_i}(q(t)), \tag{5.16}$$

$$q_i(t + \varepsilon) = q_i(t) + \varepsilon \frac{p_i(t + \varepsilon)}{m_i}. \tag{5.17}$$

We simply use the *new* value for the momentum variables, p_i, when computing the new value for the position variables, q_i. A method with similar performance can be obtained by instead updating the q_i first and using their new values to update the p_i.

Figure 5.1b shows the results using this modification of Euler's method with $\varepsilon = 0.3$. Though not perfect, the trajectory it produces is much closer to the true trajectory than that obtained using Euler's method, with no tendency to diverge to infinity. This better performance is related to the modified method's exact preservation of volume, which helps avoid divergence to infinity or spiraling into the origin, since these would typically involve the volume expanding to infinity or contracting to zero.

To see that this modification of Euler's method preserves volume exactly despite the finite discretization of time, note that both the transformation from $(q(t), p(t))$ to $(q(t), p(t + \varepsilon))$ via Equation 5.16 and the transformation from $(q(t), p(t + \varepsilon))$ to $(q(t + \varepsilon), p(t + \varepsilon))$ via Equation 5.17 are "shear" transformations, in which only some of the variables change (either the p_i or the q_i), by amounts that depend only on the variables that do not change. Any shear transformation will preserve volume, since its Jacobian matrix will have determinant one (as the only nonzero term in the determinant will be the product of diagonal elements, which will all be one).

5.2.3.3 The Leapfrog Method

Even better results can be obtained with the *leapfrog* method, which works as follows:

$$p_i\,(t + \varepsilon/2) = p_i(t) - (\varepsilon/2)\ \frac{\partial U}{\partial q_i}(q(t)), \tag{5.18}$$

$$q_i(t + \varepsilon) = q_i(t) + \varepsilon \frac{p_i(t + \varepsilon/2)}{m_i}, \tag{5.19}$$

$$p_i(t + \varepsilon) = p_i\,(t + \varepsilon/2) - (\varepsilon/2)\ \frac{\partial U}{\partial q_i}(q(t + \varepsilon)). \tag{5.20}$$

We start with a half step for the momentum variables, then do a full step for the position variables, using the new values of the momentum variables, and finally do another half step for the momentum variables, using the new values for the position variables. An analogous scheme can be used with any kinetic energy function, with $\partial K/\partial p_i$ replacing p_i/m_i above.

When we apply Equations 5.18 through 5.20 a second time to go from time $t + \varepsilon$ to $t + 2\varepsilon$, we can combine the last half step of the first update, from $p_i(t + \varepsilon/2)$ to $p_i(t + \varepsilon)$, with the first half step of the second update, from $p_i(t + \varepsilon)$ to $p_i(t + \varepsilon + \varepsilon/2)$. The leapfrog method then looks very similar to the modification of Euler's method in Equations 5.17 and 5.16, except that leapfrog performs half steps for momentum at the very beginning and very end of the trajectory, and the time labels of the momentum values computed are shifted by $\varepsilon/2$.

The leapfrog method preserves volume exactly, since Equations 5.18 through 5.20 are shear transformations. Due to its symmetry, it is also reversible by simply negating p, applying the same number of steps again, and then negating p again.

Figure 5.1c shows the results using the leapfrog method with a stepsize of $\varepsilon = 0.3$, which are indistinguishable from the true trajectory, at the scale of this plot. In Figure 5.1d, the results of using the leapfrog method with $\varepsilon = 1.2$ are shown (still with 20 steps, so almost four cycles are seen, rather than almost one). With this larger stepsize, the approximation error is clearly visible, but the trajectory still remains stable (and will stay stable indefinitely). Only when the stepsize approaches $\varepsilon = 2$ do the trajectories become unstable.

5.2.3.4 Local and Global Error of Discretization Methods

I will briefly discuss how the error from discretizing the dynamics behaves in the limit as the stepsize, ε, goes to zero; Leimkuhler and Reich (2004) provide a much more detailed discussion. For useful methods, the error goes to zero as ε goes to zero, so that any upper limit on the error will apply (apart from a usually unknown constant factor) to any differentiable function of state—for example, if the error for (q, p) is no more than order ε^2, the error for $H(q, p)$ will also be no more than order ε^2.

The *local error* is the error after one step, that moves from time t to time $t + \varepsilon$. The *global error* is the error after simulating for some fixed time interval, s, which will require s/ε steps. If the local error is order ε^p, the global error will be order ε^{p-1}—the local errors of order ε^p accumulate over the s/ε steps to give an error of order ε^{p-1}. If we instead fix ε and consider increasing the time, s, for which the trajectory is simulated, the error can in general increase exponentially with s. Interestingly, however, this is often not what happens when simulating Hamiltonian dynamics with a symplectic method, as can be seen in Figure 5.1.

The Euler method and its modification above have order ε^2 local error and order ε global error. The leapfrog method has order ε^3 local error and order ε^2 global error. As shown by Leimkuhler and Reich (2004, Section 4.3.3), this difference is a consequence of leapfrog being reversible, since any reversible method must have global error that is of even order in ε.

5.3 MCMC from Hamiltonian Dynamics

Using Hamiltonian dynamics to sample from a distribution requires translating the density function for this distribution to a potential energy function and introducing "momentum" variables to go with the original variables of interest (now seen as "position" variables). We can then simulate a Markov chain in which each iteration resamples the momentum and then does a Metropolis update with a proposal found using Hamiltonian dynamics.

5.3.1 Probability and the Hamiltonian: Canonical Distributions

The distribution we wish to sample can be related to a potential energy function via the concept of a *canonical distribution* from statistical mechanics. Given some energy function, $E(x)$, for the state, x, of some physical system, the canonical distribution over states has probability or probability density function

$$P(x) = \frac{1}{Z} \exp\left(\frac{-E(x)}{T}\right). \tag{5.21}$$

Here, T is the temperature of the system,* and Z is the normalizing constant needed for this function to sum or integrate to one. Viewing this the opposite way, if we are interested in some distribution with density function $P(x)$, we can obtain it as a canonical distribution with $T = 1$ by setting $E(x) = -\log P(x) - \log Z$, where Z is any convenient positive constant.

The Hamiltonian is an energy function for the joint state of "position," q, and "momentum," p, and so defines a joint distribution for them as follows:

$$P(q,p) = \frac{1}{Z} \exp\left(\frac{-H(q,p)}{T}\right).$$

Note that the invariance of H under Hamiltonian dynamics means that a Hamiltonian trajectory will (if simulated exactly) move within a hypersurface of constant probability density.

If $H(q,p) = U(q) + K(p)$, the joint density is

$$P(q,p) = \frac{1}{Z} \exp\left(\frac{-U(q)}{T}\right) \exp\left(\frac{-K(p)}{T}\right), \tag{5.22}$$

and we see that q and p are independent, and each have canonical distributions, with energy functions $U(q)$ and $K(p)$. We will use q to represent the variables of interest, and introduce p just to allow Hamiltonian dynamics to operate.

In Bayesian statistics, the posterior distribution for the model parameters is the usual focus of interest, and hence these parameters will take the role of the position, q. We can express the posterior distribution as a canonical distribution (with $T = 1$) using a potential energy function defined as

$$U(q) = -\log\left[\pi(q)L(q \mid D)\right],$$

where $\pi(q)$ is the prior density, and $L(q|D)$ is the likelihood function given data D.

5.3.2 The Hamiltonian Monte Carlo Algorithm

We now have the background needed to present the Hamiltonian Monte Carlo algorithm. HMC can be used to sample only from continuous distributions on $\mathbb{R}^d$ for which the density function can be evaluated (perhaps up to an unknown normalizing constant). For the moment, I will also assume that the density is nonzero everywhere (but this is relaxed in Section 5.5.1). We must also be able to compute the partial derivatives of the log of the density function. These derivatives must therefore exist, except perhaps on a set of points with probability zero, for which some arbitrary value could be returned.

HMC samples from the canonical distribution for q and p defined by Equation 5.22, in which q has the distribution of interest, as specified using the potential energy function $U(q)$. We can choose the distribution of the momentum variables, p, which are independent of q, as we wish, specifying the distribution via the kinetic energy function, $K(p)$. Current practice with HMC is to use a quadratic kinetic energy, as in Equation 5.5, which leads p to have a zero-mean multivariate Gaussian distribution. Most often, the components of

* Note to physicists: I assume here that temperature is measured in units that make Boltzmann's constant unity.

p are specified to be independent, with component i having variance m_i. The kinetic energy function producing this distribution (setting $T = 1$) is

$$K(p) = \sum_{i=1}^{d} \frac{p_i^2}{2m_i}. \tag{5.23}$$

We will see in Section 5.4 how the choice for the m_i affects performance.

5.3.2.1 The Two Steps of the HMC Algorithm

Each iteration of the HMC algorithm has two steps. The first changes only the momentum; the second may change both position and momentum. Both steps leave the canonical joint distribution of (q, p) invariant, and hence their combination also leaves this distribution invariant.

In the first step, new values for the momentum variables are randomly drawn from their Gaussian distribution, independently of the current values of the position variables. For the kinetic energy of Equation 5.23, the d momentum variables are independent, with p_i having mean zero and variance m_i. Since q is not changed, and p is drawn from its correct conditional distribution given q (the same as its marginal distribution, due to independence), this step obviously leaves the canonical joint distribution invariant.

In the second step, a Metropolis update is performed, using Hamiltonian dynamics to propose a new state. Starting with the current state, (q, p), Hamiltonian dynamics is simulated for L steps using the leapfrog method (or some other reversible method that preserves volume), with a stepsize of ε. Here, L and ε are parameters of the algorithm, which need to be tuned to obtain good performance (as discussed below in Section 5.4.2). The momentum variables at the end of this L-step trajectory are then negated, giving a proposed state (q^*, p^*). This proposed state is accepted as the next state of the Markov chain with probability

$$\min\left[1, \exp(-H(q^*, p^*) + H(q, p))\right] = \min\left[1, \exp(-U(q^*) + U(q) - K(p^*) + K(p))\right].$$

If the proposed state is not accepted (i.e. it is rejected), the next state is the same as the current state (and is counted again when estimating the expectation of some function of state by its average over states of the Markov chain). The negation of the momentum variables at the end of the trajectory makes the Metropolis proposal symmetrical, as needed for the acceptance probability above to be valid. This negation need not be done in practice, since $K(p) = K(-p)$, and the momentum will be replaced before it is used again, in the first step of the next iteration. (This assumes that these HMC updates are the only ones performed.)

If we look at HMC as sampling from the joint distribution of q and p, the Metropolis step using a proposal found by Hamiltonian dynamics leaves the probability density for (q, p) unchanged or almost unchanged. Movement to (q, p) points with a different probability density is accomplished only by the first step in an HMC iteration, in which p is replaced by a new value. Fortunately, this replacement of p can change the probability density for (q, p) by a large amount, so movement to points with a different probability density is not a problem (at least not for this reason). Looked at in terms of q only, Hamiltonian dynamics for (q, p) can produce a value for q with a much different probability density (equivalently, a much different potential energy, $U(q)$). However, the resampling of the momentum variables is still crucial to obtaining the proper distribution for q. Without resampling, $H(q, p) = U(q) + K(p)$ will be (nearly) constant, and since $K(p)$ and $U(q)$ are

```
HMC = function (U, grad_U, epsilon, L, current_q)
{
  q = current_q
  p = rnorm(length(q),0,1)  # independent standard normal variates
  current_p = p

  # Make a half step for momentum at the beginning
  p = p - epsilon * grad_U(q) / 2

  # Alternate full steps for position and momentum

  for (i in 1:L)
  {
    # Make a full step for the position
    q = q + epsilon * p
    # Make a full step for the momentum, except at end of trajectory
    if (i!=L) p = p - epsilon * grad_U(q)
  }

  # Make a half step for momentum at the end.
  p = p - epsilon * grad_U(q) / 2
  # Negate momentum at end of trajectory to make the proposal symmetric
  p = -p

  # Evaluate potential and kinetic energies at start and end of trajectory

  current_U = U(current_q)
  current_K = sum(current_p^2) / 2
  proposed_U = U(q)
  proposed_K = sum(p^2) / 2

  # Accept or reject the state at end of trajectory, returning either
  # the position at the end of the trajectory or the initial position

  if (runif(1) < exp(current_U-proposed_U+current_K-proposed_K))
  {
    return (q)  # accept
  }
  else
  {
    return (current_q)  # reject
  }
}
```

FIGURE 5.2
The Hamiltonian Monte Carlo algorithm.

nonnegative, $U(q)$ could never exceed the initial value of $H(q,p)$ if no resampling for p were done.

A function that implements a single iteration of the HMC algorithm, written in the R language,* is shown in Figure 5.2. Its first two arguments are functions: `U`, which returns

* R is available for free from www.r-project.org

the potential energy given a value for q, and `grad_U`, which returns the vector of partial derivatives of U given q. Other arguments are the stepsize, `epsilon`, for leapfrog steps; the number of leapfrog steps in the trajectory, `L`; and the current position, `current_q`, that the trajectory starts from. Momentum variables are sampled within this function, and discarded at the end, with only the next position being returned. The kinetic energy is assumed to have the simplest form, $K(p) = \sum p_i^2/2$ (i.e. all m_i are one). In this program, all components of p and of q are updated simultaneously, using vector operations. This simple implementation of HMC is available from my web page,* along with other R programs with extra features helpful for practical use, and that illustrate some of the variants of HMC in Section 5.5.

5.3.2.2 Proof That HMC Leaves the Canonical Distribution Invariant

The Metropolis update above is reversible with respect to the canonical distribution for q and p (with $T = 1$), a condition also known as "detailed balance," and which can be phrased informally as follows. Suppose that we partition the (q, p) space into regions A_k, each with the same small volume V. Let the image of A_k with respect to the operation of L leapfrog steps, plus a negation of the momentum, be B_k. Due to the reversibility of the leapfrog steps, the B_k will also partition the space, and since the leapfrog steps preserve volume (as does negation), each B_k will also have volume V. Detailed balance holds if, for all i and j,

$$P(A_i)T(B_j \mid A_i) = P(B_j)T(A_i \mid B_j), \tag{5.24}$$

where P is probability under the canonical distribution, and $T(X|Y)$ is the conditional probability of proposing and then accepting a move to region X if the current state is in region Y. Clearly, when $i \neq j$, $T(A_i \mid B_j) = T(B_j \mid A_i) = 0$ and so Equation 5.24 will be satisfied. Since the Hamiltonian is continuous almost everywhere, in the limit as the regions A_k and B_k become smaller, the Hamiltonian becomes effectively constant within each region, with value H_X in region X, and hence the canonical probability density and the transition probabilities become effectively constant within each region as well. We can now rewrite Equation 5.24 for $i = j$ (say, both equal to k) as

$$\frac{V}{Z}\exp(-H_{A_k})\min\left[1, \exp(-H_{B_k}+H_{A_k})\right] = \frac{V}{Z}\exp(-H_{B_k})\min\left[1, \exp(-H_{A_k}+H_{B_k})\right],$$

which is easily seen to be true.

Detailed balance implies that this Metropolis update leaves the canonical distribution for q and p invariant. This can be seen as follows. Let $R(X)$ be the probability that the Metropolis update for a state in the small region X leads to rejection of the proposed state. Suppose that the current state is distributed according to the canonical distribution. The probability that the next state is in a small region B_k is the sum of the probability that the current state is in B_k and the update leads to rejection, and the probability that the current state is in some region from which a move to B_k is proposed and accepted. The probability of the next state

* www.cs.utoronto.ca/∼radford

being in B_k can therefore be written as

$$\begin{aligned} P(B_k)R(B_k) + \sum_i P(A_i)T(B_k|A_i) &= P(B_k)R(B_k) + \sum_i P(B_k)T(A_i|B_k) \\ &= P(B_k)R(B_k) + P(B_k)\sum_i T(A_i|B_k) \\ &= P(B_k)R(B_k) + P(B_k)(1 - R(B_k)) \\ &= P(B_k). \end{aligned}$$

The Metropolis update within HMC therefore leaves the canonical distribution invariant.

Since both the sampling of momentum variables and the Metropolis update with a proposal found by Hamiltonian dynamics leave the canonical distribution invariant, the HMC algorithm as a whole does as well.

5.3.2.3 Ergodicity of HMC

Typically, the HMC algorithm will also be "ergodic"—it will not be trapped in some subset of the state space, and hence will asymptotically converge to its (unique) invariant distribution. In an HMC iteration, any value can be sampled for the momentum variables, which can typically then affect the position variables in arbitrary ways. However, ergodicity can fail if the L leapfrog steps in a trajectory produce an exact periodicity for some function of state. For example, with the simple Hamiltonian of Equation 5.8, the exact solutions (given by Equation 5.9) are periodic with period 2π. Approximate trajectories found with L leapfrog steps with stepsize ε may return to the same position coordinate when $L\varepsilon$ is approximately 2π. HMC with such values for L and ε will not be ergodic. For nearby values of L and ε, HMC may be theoretically ergodic, but take a very long time to move about the full state space.

This potential problem of nonergodicity can be solved by randomly choosing ε or L (or both) from some fairly small interval (Mackenzie, 1989). Doing this routinely may be advisable. Although in real problems interactions between variables typically prevent any exact periodicities from occurring, near periodicities might still slow HMC considerably.

5.3.3 Illustrations of HMC and Its Benefits

I will now illustrate some practical issues with HMC, and demonstrate its potential to sample much more efficiently than simple methods such as random-walk Metropolis. I use simple Gaussian distributions for these demonstrations, so that the results can be compared with known values, but of course HMC is typically used for more complex distributions.

5.3.3.1 Trajectories for a Two-Dimensional Problem

Consider sampling from a distribution for two variables that is bivariate Gaussian, with means of zero, standard deviations of one, and correlation 0.95. We regard these as "position" variables, and introduce two corresponding "momentum" variables, defined to have a Gaussian distribution with means of zero, standard deviations of one, and zero correlation. We then define the Hamiltonian as

$$H(q,p) = q^T \Sigma^{-1} q/2 + p^T p/2, \quad \text{with } \Sigma = \begin{bmatrix} 1 & 0.95 \\ 0.95 & 1 \end{bmatrix}.$$

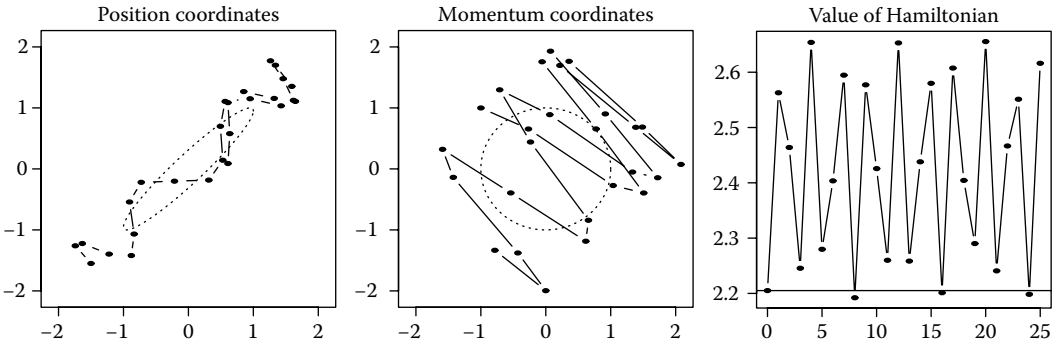

FIGURE 5.3
A trajectory for a two-dimensional Gaussian distribution, simulated using 25 leapfrog steps with a stepsize of 0.25. The ellipses plotted are one standard deviation from the means. The initial state had $q = [-1.50, -1.55]^T$ and $p = [-1, 1]^T$.

Figure 5.3 shows a trajectory based on this Hamiltonian, such as might be used to propose a new state in the HMC method, computed using $L = 25$ leapfrog steps, with a stepsize of $\varepsilon = 0.25$. Since the full state space is four-dimensional, Figure 5.3 shows the two position coordinates and the two momentum coordinates in separate plots, while the third plot shows the value of the Hamiltonian after each leapfrog step.

Notice that this trajectory does not resemble a random walk. Instead, starting from the lower left-hand corner, the position variables systematically move upward and to the right, until they reach the upper right-hand corner, at which point the direction of motion is reversed. The consistency of this motion results from the role of the momentum variables. The projection of p in the diagonal direction will change only slowly, since the gradient in that direction is small, and hence the direction of diagonal motion stays the same for many leapfrog steps. While this large-scale diagonal motion is happening, smaller-scale oscillations occur, moving back and forth across the "valley" created by the high correlation between the variables.

The need to keep these smaller oscillations under control limits the stepsize that can be used. As can be seen in the rightmost plot in Figure 5.3, there are also oscillations in the value of the Hamiltonian (which would be constant if the trajectory were simulated exactly). If a larger stepsize were used, these oscillations would be larger. At a critical stepsize ($\varepsilon = 0.45$ in this example), the trajectory becomes unstable, and the value of the Hamiltonian grows without bound. As long as the stepsize is less than this, however, the error in the Hamiltonian stays bounded regardless of the number of leapfrog steps done. This lack of growth in the error is not guaranteed for all Hamiltonians, but it does hold for many distributions more complex than Gaussians. As can be seen, however, the error in the Hamiltonian along the trajectory does tend to be positive more often than negative. In this example, the error is $+0.41$ at the end of the trajectory, so if this trajectory were used for an HMC proposal, the probability of accepting the endpoint as the next state would be $\exp(-0.41) = 0.66$.

5.3.3.2 Sampling from a Two-Dimensional Distribution

Figures 5.4 and 5.5 show the results of using HMC and a simple random-walk Metropolis method to sample from a bivariate Gaussian similar to the one just discussed, but with stronger correlation of 0.98.

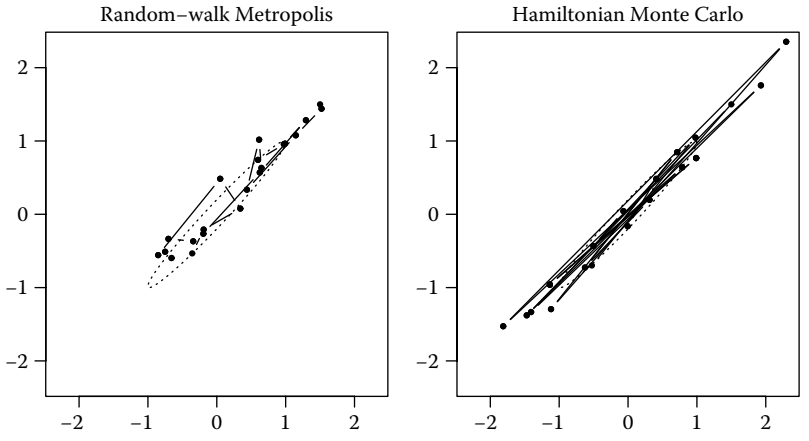

FIGURE 5.4
Twenty iterations of the random-walk Metropolis method (with 20 updates per iteration) and of the Hamiltonian Monte Carlo method (with 20 leapfrog steps per trajectory) for a two-dimensional Gaussian distribution with marginal standard deviations of one and correlation 0.98. Only the two position coordinates are plotted, with ellipses drawn one standard deviation away from the mean.

In this example, as in the previous one, HMC used a kinetic energy (defining the momentum distribution) of $K(p) = p^T p/2$. The results of 20 HMC iterations, using trajectories of $L = 20$ leapfrog steps with stepsize $\varepsilon = 0.18$, are shown in the right plot of Figure 5.4. These values were chosen so that the trajectory length, εL, is sufficient to move to a distant point in the distribution, without being so large that the trajectory will often waste computation time by doubling back on itself. The rejection rate for these trajectories was 0.09.

Figure 5.4 also shows every 20th state from 400 iterations of random-walk Metropolis, with a bivariate Gaussian proposal distribution with the current state as mean, zero correlation, and the same standard deviation for the two coordinates. The standard deviation of the proposals for this example was 0.18, which is the same as the stepsize used for HMC proposals, so that the change in state in these random-walk proposals was comparable to that for a single leapfrog step for HMC. The rejection rate for these random-walk proposals was 0.37.

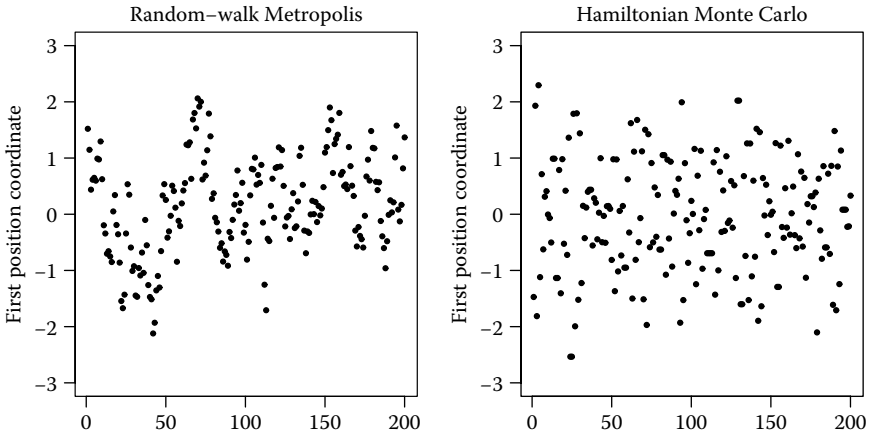

FIGURE 5.5
Two hundred iterations, starting with the 20 iterations shown above, with only the first position coordinate plotted.

One can see in Figure 5.4 how the systematic motion during an HMC trajectory (illustrated in Figure 5.3) produces larger changes in state than a corresponding number of random-walk Metropolis iterations. Figure 5.5 illustrates this difference for longer runs of 20×200 random-walk Metropolis iterations and of 200 HMC iterations.

5.3.3.3 The Benefit of Avoiding Random Walks

Avoidance of random-walk behavior, as illustrated above, is one major benefit of HMC. In this example, because of the high correlation between the two position variables, keeping the acceptance probability for random-walk Metropolis reasonably high requires that the changes proposed have a magnitude comparable to the standard deviation in the most constrained direction (0.14 in this example, the square root of the smallest eigenvalue of the covariance matrix). The changes produced using one Gibbs sampling scan would be of similar magnitude. The number of iterations needed to reach a state almost independent of the current state is mostly determined by how long it takes to explore the less constrained direction, which for this example has standard deviation 1.41—about ten times greater than the standard deviation in the most constrained direction. We might therefore expect that we would need around 10 iterations of random-walk Metropolis in which the proposal was accepted to move to a nearly independent state. But the number needed is actually roughly the square of this—around 100 iterations with accepted proposals—because the random-walk Metropolis proposals have no tendency to move consistently in the same direction.

To see this, note that the variance of the position after n iterations of random-walk Metropolis from some start state will grow in proportion to n (until this variance becomes comparable to the overall variance of the state), since the position is the sum of mostly independent movements for each iteration. The *standard deviation* of the amount moved (which gives the typical amount of movement) is therefore proportional to $\sqrt{n}$.

The stepsize used for the leapfrog steps is similarly limited by the most constrained direction, but the movement will be in the same direction for many steps. The distance moved after n steps will therefore tend to be proportional to n, until the distance moved becomes comparable to the overall width of the distribution. The advantage compared to movement by a random walk will be a factor roughly equal to the ratio of the standard deviations in the least confined direction and most confined direction—about 10 here.

Because avoiding a random walk is so beneficial, the optimal standard deviation for random-walk Metropolis proposals in this example is actually much larger than the value of 0.18 used here. A proposal standard deviation of 2.0 gives a very low acceptance rate (0.06), but this is more than compensated for by the large movement (to a nearly independent point) on the rare occasions when a proposal is accepted, producing a method that is about as efficient as HMC. However, this strategy of making large changes with a small acceptance rate works only when, as here, the distribution is tightly constrained in only one direction.

5.3.3.4 Sampling from a 100-Dimensional Distribution

More typical behavior of HMC and random-walk Metropolis is illustrated by a 100-dimensional multivariate Gaussian distribution in which the variables are independent, with means of zero, and standard deviations of 0.01, 0.02, ..., 0.99, 1.00. Suppose that we have no knowledge of the details of this distribution, so we will use HMC with the same simple, rotationally symmetric kinetic energy function as above, $K(p) = p^T p/2$, and use random-walk Metropolis proposals in which changes to each variable are independent, all

with the same standard deviation. As discussed below in Section 5.4.1, the performance of both these sampling methods is invariant to rotation, so this example is illustrative of how they perform on any multivariate Gaussian distribution in which the square roots of the eigenvalues of the covariance matrix are $0.01, 0.02, \ldots, 0.99, 1.00$.

For this problem, the position coordinates, q_i, and corresponding momentum coordinates, p_i, are all independent, so the leapfrog steps used to simulate a trajectory operate independently for each (q_i, p_i) pair. However, whether the trajectory is accepted depends on the total error in the Hamiltonian due to the leapfrog discretization, which is a sum of the errors due to each (q_i, p_i) pair (for the terms in the Hamiltonian involving this pair). Keeping this error small requires limiting the leapfrog stepsize to a value roughly equal to the smallest of the standard deviations (0.01), which implies that many leapfrog steps will be needed to move a distance comparable to the largest of the standard deviations (1.00).

Consistent with this, I applied HMC to this distribution using trajectories with $L = 150$ and with ε randomly selected for each iteration, uniformly from $(0.0104, 0.0156)$, which is $0.013 \pm 20\%$. I used random-walk Metropolis with proposal standard deviation drawn uniformly from $(0.0176, 0.0264)$, which is $0.022 \pm 20\%$. These are close to optimal settings for both methods. The rejection rate was 0.13 for HMC and 0.75 for random-walk Metropolis.

Figure 5.6 shows results from runs of 1000 iterations of HMC (right) and of random-walk Metropolis (left), counting 150 random-walk Metropolis updates as one iteration, so that the computation time per iteration is comparable to that for HMC. The plot shows the last variable, with the largest standard deviation. The autocorrelation of these values is clearly much higher for random-walk Metropolis than for HMC. Figure 5.7 shows the estimates for the mean and standard deviation of each of the 100 variables obtained using the HMC and random-walk Metropolis runs (estimates were just the sample means and sample standard deviations of the values from the 1000 iterations). Except for the first few

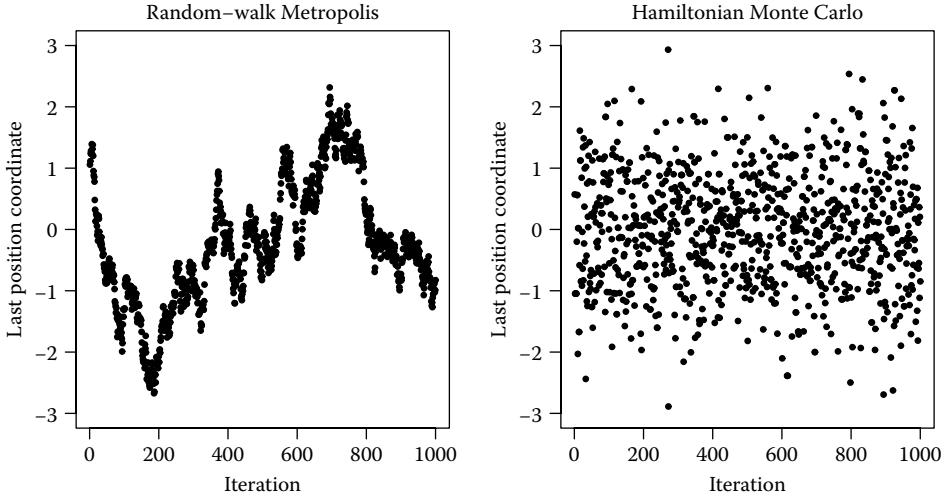

FIGURE 5.6
Values for the variable with largest standard deviation for the 100-dimensional example, from a random-walk Metropolis run and an HMC run with $L = 150$. To match computation time, 150 updates were counted as one iteration for random-walk Metropolis.

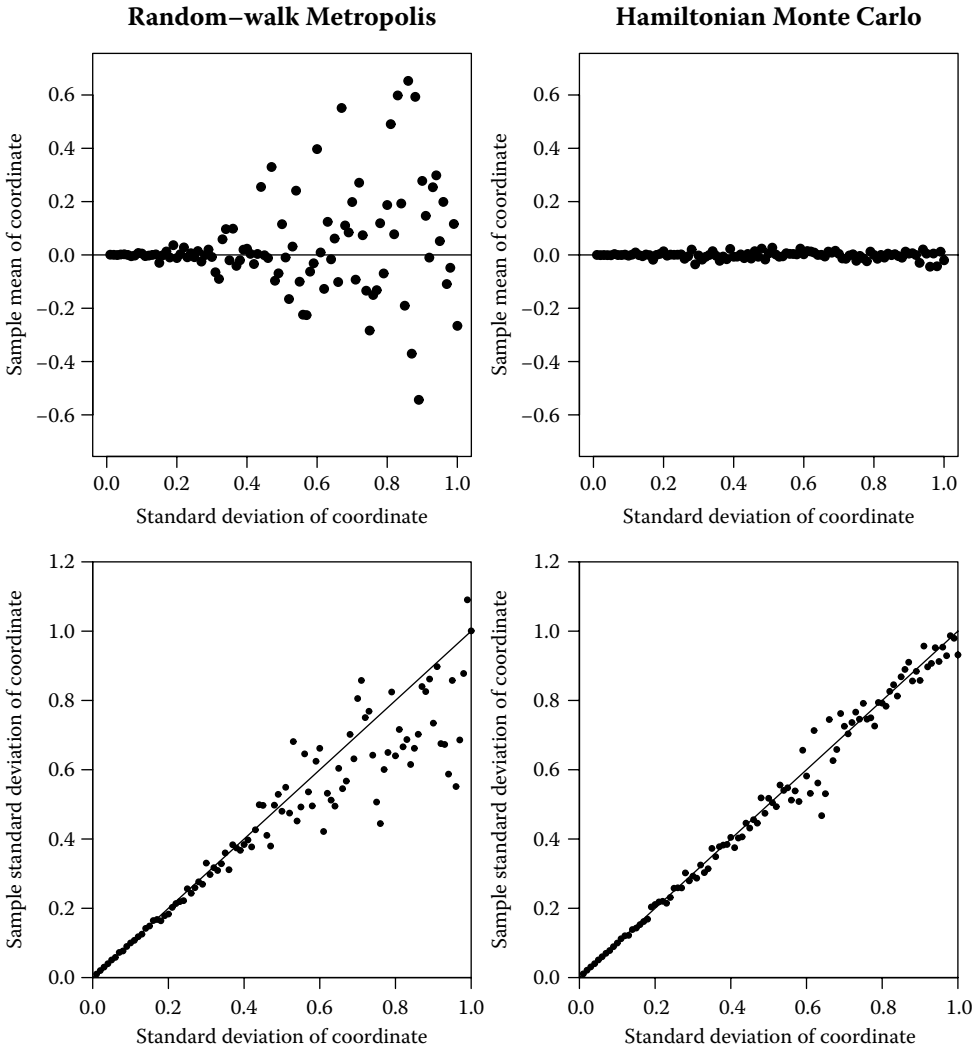

FIGURE 5.7
Estimates of means (top) and standard deviations (bottom) for the 100-dimensional example, using random-walk Metropolis (left) and HMC (right). The 100 variables are labeled on the horizontal axes by the true standard deviaton of that variable. Estimates are on the vertical axes.

variables (with smallest standard deviations), the error in the mean estimates from HMC is roughly 10 times less than the error in the mean estimates from random-walk Metropolis. The standard deviation estimates from HMC are also better.

The randomization of the leapfrog stepsize done in this example follows the advice discussed at the end of Section 5.3.2. In this example, not randomizing the stepsize (fixing $\varepsilon = 0.013$) does in fact cause problems—the variables with standard deviations near 0.31 or 0.62 change only slowly, since 150 leapfrog steps with $\epsilon = 0.013$ produces nearly a full or half cycle for these variables, so an accepted trajectory does not make much of a change in the absolute value of the variable.

5.4 HMC in Practice and Theory

Obtaining the benefits from HMC illustrated in the previous section, including random-walk avoidance, requires proper tuning of L and ε. I discuss tuning of HMC below, and also show how performance can be improved by using whatever knowledge is available regarding the scales of variables and their correlations. After briefly discussing what to do when HMC alone is not enough, I discuss an additional benefit of HMC—its better scaling with dimensionality than simple Metropolis methods.

5.4.1 Effect of Linear Transformations

Like all MCMC methods I am aware of, the performance of HMC may change if the variables being sampled are transformed by multiplication by some nonsingular matrix, A. However, performance stays the same (except perhaps in terms of computation time per iteration) if at the same time the corresponding momentum variables are multiplied by $(A^T)^{-1}$. These facts provide insight into the operation of HMC, and can help us improve performance when we have some knowledge of the scales and correlations of the variables.

Let the new variables be $q' = Aq$. The probability density for q' will be given by $P'(q') = P(A^{-1}q')/|\det(A)|$, where $P(q)$ is the density for q. If the distribution for q is the canonical distribution for a potential energy function $U(q)$ (see Section 5.3.1), we can obtain the distribution for q' as the canonical distribution for $U'(q') = U(A^{-1}q')$. (Since $|\det(A)|$ is a constant, we need not include a $\log|\det(A)|$ term in the potential energy.)

We can choose whatever distribution we wish for the corresponding momentum variables, so we could decide to use the same kinetic energy as before. Alternatively, we can choose to transform the momentum variables by $p' = (A^T)^{-1}p$, and use a new kinetic energy of $K'(p') = K(A^Tp')$. If we were using a quadratic kinetic energy, $K(p) = p^TM^{-1}p/2$ (see Equation 5.5), the new kinetic energy will be

$$K'(p') = (A^Tp')^TM^{-1}(A^Tp')/2 = (p')^T(A\,M^{-1}A^T)\,p'/2 = (p')^T(M')^{-1}p'/2, \tag{5.25}$$

where $M' = (A\,M^{-1}A^T)^{-1} = (A^{-1})^TMA^{-1}$.

If we use momentum variables transformed in this way, the dynamics for the new variables, (q', p'), essentially replicates the original dynamics for (q, p), so the performance of HMC will be the same. To see this, note that if we follow Hamiltonian dynamics for (q', p'), the result in terms of the original variables will be as follows (see Equations 5.6 and 5.7):

$$\frac{dq}{dt} = A^{-1}\,\frac{dq'}{dt} = A^{-1}(M')^{-1}\,p' = A^{-1}(A\,M^{-1}A^T)(A^T)^{-1}\,p = M^{-1}\,p,$$

$$\frac{dp}{dt} = A^T\,\frac{dp'}{dt} = -A^T\,\nabla U'(q') = -A^T\,(A^{-1})^T\,\nabla U(A^{-1}q') = -\nabla U(q),$$

which matches what would happen following Hamiltonian dynamics for (q, p).

If A is an orthogonal matrix (such as a rotation matrix), for which $A^{-1} = A^T$, the performance of HMC is unchanged if we transform both q and p by multiplying by A (since $(A^T)^{-1} = A$). If we chose a rotationally symmetric distribution for the momentum, with $M = mI$ (i.e. the momentum variables are independent, each having variance m), such an orthogonal transformation will not change the kinetic energy function (and hence not change the distribution of the momentum variables), since we will have $M' = (A\,(mI)^{-1}A^T)^{-1} = mI$.

Such an invariance to rotation holds also for a random-walk Metropolis method in which the proposal distribution is rotationally symmetric (e.g. Gaussian with covariance matrix mI). In contrast, Gibbs sampling is not rotationally invariant, nor is a scheme in which the Metropolis algorithm is used to update each variable in turn (with a proposal that changes only that variable). However, Gibbs sampling is invariant to rescaling of the variables (transformation by a diagonal matrix), which is not true for HMC or random-walk Metropolis, unless the kinetic energy or proposal distribution is transformed in a corresponding way.

Suppose that we have an estimate, Σ, of the covariance matrix for q, and suppose also that q has at least a roughly Gaussian distribution. How can we use this information to improve the performance of HMC? One way is to transform the variables so that their covariance matrix is close to the identity, by finding the Cholesky decomposition, $\Sigma = LL^T$, with L being lower-triangular, and letting $q' = L^{-1}q$. We then let our kinetic energy function be $K(p) = p^T p/2$. Since the momentum variables are independent, and the position variables are close to independent with variances close to one (if our estimate Σ and our assumption that q is close to Gaussian are good), HMC should perform well using trajectories with a small number of leapfrog steps, which will move all variables to a nearly independent point. More realistically, the estimate Σ may not be very good, but this transformation could still improve performance compared to using the same kinetic energy with the original q variables.

An equivalent way to make use of the estimated covariance Σ is to keep the original q variables, but use the kinetic energy function $K(p) = p^T \Sigma p/2$—that is, we let the momentum variables have covariance Σ^{-1}. The equivalence can be seen by transforming this kinetic energy to correspond to a transformation to $q' = L^{-1}q$ (see Equation 5.25), which gives $K(p') = (p')^T M'^{-1} p'$ with $M' = (L^{-1}(LL^T)(L^{-1})^T)^{-1} = I$.

Using such a kinetic energy function to compensate for correlations between position variables has a long history in molecular dynamics (Bennett, 1975). The usefulness of this technique is limited by the computational cost of matrix operations when the dimensionality is high.

Using a diagonal Σ can be feasible even in high-dimensional problems. Of course, this provides information only about the different scales of the variables, not their correlation. Moreover, when the actual correlations are nonzero, it is not clear what scales to use. Making an optimal choice is probably infeasible. Some approximation to the conditional standard deviation of each variable given all the others may be possible—as I have done for Bayesian neural network models (Neal, 1996a). If this also is not feasible, using approximations to the marginal standard deviations of the variables may be better than using the same scale for them all.

5.4.2 Tuning HMC

One practical impediment to the use of Hamiltonian Monte Carlo is the need to select suitable values for the leapfrog stepsize, ε, and the number of leapfrog steps, L, which together determine the length of the trajectory in fictitious time, εL. Most MCMC methods have parameters that need to be tuned, with the notable exception of Gibbs sampling when the conditional distributions are amenable to direct sampling. However, tuning HMC is more difficult in some respects than tuning a simple Metropolis method.

5.4.2.1 Preliminary Runs and Trace Plots

Tuning HMC will usually require preliminary runs with trial values for ε and L. In judging how well these runs work, trace plots of quantities that are thought to be indicative

of overall convergence should be examined. For Bayesian inference problems, high-level hyperparameters are often among the slowest-moving quantities. The value of the potential energy function, $U(q)$, is also usually of central significance. The autocorrelation for such quantities indicates how well the Markov chain is exploring the state space. Ideally, we would like the state after one HMC iteration to be nearly independent of the previous state.

Unfortunately, preliminary runs can be misleading, if they are not long enough to have reached equilibrium. It is possible that the best choices of ε and L for reaching equilibrium are different from the best choices once equilibrium is reached, and even at equilibrium, it is possible that the best choices vary from one place to another. If necessary, at each iteration of HMC, ε and L can be chosen randomly from a selection of values that are appropriate for different parts of the state space (or these selections and can be used sequentially).

Doing several runs with different random starting states is advisable (for both preliminary and final runs), so that problems with isolated modes can be detected. Note that HMC is no less (or more) vulnerable to problems with isolated modes than other MCMC methods that make local changes to the state. If isolated modes are found to exist, something needs to be done to solve this problem—just combining runs that are each confined to a single mode is not valid. A modification of HMC with "tempering" along a trajectory (Section 5.5.7) can sometimes help with multiple modes.

5.4.2.2 What Stepsize?

Selecting a suitable leapfrog stepsize, ε, is crucial. Too large a stepsize will result in a very low acceptance rate for states proposed by simulating trajectories. Too small a stepsize will either waste computation time, by the same factor as the stepsize is too small, or (worse) will lead to slow exploration by a random walk, if the trajectory length, εL, is then too short (i.e. L is not large enough; see below).

Fortunately, as illustrated in Figure 5.3, the choice of stepsize is almost independent of how many leapfrog steps are done. The error in the value of the Hamiltonian (which will determine the rejection rate) usually does not increase with the number of leapfrog steps, *provided* that the stepsize is small enough that the dynamics is stable.

The issue of stability can be seen in a simple one-dimensional problem in which the following Hamiltonian is used:

$$H(q,p) = \frac{q^2}{2\sigma^2} + \frac{p^2}{2}.$$

The distribution for q that this defines is Gaussian with standard deviation σ. A leapfrog step for this system (as for any quadratic Hamiltonian) will be a linear mapping from $(q(t), p(t))$ to $(q(t+\varepsilon), p(t+\varepsilon))$. Referring to Equations 5.18 through 5.20, we see that this mapping can be represented by a matrix multiplication as follows:

$$\begin{bmatrix} q(t+\varepsilon) \\ p(t+\varepsilon) \end{bmatrix} = \begin{bmatrix} 1 - \varepsilon^2/2\sigma^2 & \varepsilon \\ -\varepsilon/\sigma^2 + \varepsilon^3/4\sigma^4 & 1 - \varepsilon^2/2\sigma^2 \end{bmatrix} \begin{bmatrix} q(t) \\ p(t) \end{bmatrix}.$$

Whether iterating this mapping leads to a stable trajectory, or one that diverges to infinity, depends on the magnitudes of the eigenvalues of the above matrix, which are

$$\left(1 - \frac{\varepsilon^2}{2\sigma^2}\right) \pm \left(\frac{\varepsilon}{\sigma}\right) \sqrt{\varepsilon^2/4\sigma^2 - 1}.$$

When $\varepsilon/\sigma > 2$, these eigenvalues are real, and at least one will have absolute value greater than one. Trajectories computed using the leapfrog method with this ε will therefore be unstable. When $\varepsilon/\sigma < 2$, the eigenvalues are complex, and both have squared magnitude of

$$\left(1 - \frac{\varepsilon^2}{2\sigma^2}\right)^2 + \left(\frac{\varepsilon^2}{\sigma^2}\right)\left(1 - \frac{\varepsilon^2}{4\sigma^2}\right) = 1.$$

Trajectories computed with $\varepsilon < 2\sigma$ are therefore stable.

For multidimensional problems in which the kinetic energy used is $K(p) = p^T p/2$ (as in the example above), the stability limit for ε will be determined (roughly) by the width of the distribution in the most constrained direction—for a Gaussian distribution, this would the square root of the smallest eigenvalue of the covariance matrix for q. Stability for more general quadratic Hamiltonians with $K(p) = p^T M^{-1} p/2$ can be determined by applying a linear transformation that makes $K(p') = (p')^T p'/2$, as discussed above in Section 5.4.1.

When a stepsize, ε, that produces unstable trajectories is used, the value of H grows exponentially with L, and consequently the acceptance probability will be extremely small. For low-dimensional problems, using a value for ε that is just a little below the stability limit is sufficient to produce a good acceptance rate. For high-dimensional problems, however, the stepsize may need to be reduced further than this to keep the error in H to a level that produces a good acceptance probability. This is discussed further in Section 5.4.4.

Choosing too large a value of ε can have very bad effects on the performance of HMC. In this respect, HMC is more sensitive to tuning than random-walk Metropolis. A standard deviation for proposals needs to be chosen for random-walk Metropolis, but performance degrades smoothly as this choice is made too large, without the sharp degradation seen with HMC when ε exceeds the stability limit. (However, in high-dimensional problems, the degradation in random-walk Metropolis with too large a proposal standard deviation can also be quite sharp, so this distinction becomes less clear.)

This sharp degradation in performance of HMC when the stepsize is too big would not be a serious issue if the stability limit were constant—the problem would be obvious from preliminary runs, and so could be fixed. The real danger is that the stability limit may differ for several regions of the state space that all have substantial probability. If the preliminary runs are started in a region where the stability limit is large, a choice of ε a little less than this limit might appear to be appropriate. However, if this ε is above the stability limit for some other region, the runs may never visit this region, even though it has substantial probability, producing a drastically wrong result. To see why this could happen, note that if the run ever does visit the region where the chosen ε would produce instability, it will stay there for a very long time, since the acceptance probability with that ε will be very small. Since the method nevertheless leaves the correct distribution invariant, it follows that the run only rarely moves to this region from a region where the chosen ε leads to stable trajectories. One simple context where this problem can arise is when sampling from a distribution with very light tails (lighter than a Gaussian distribution), for which the log of the density will fall faster than quadratically. In the tails, the gradient of the log density will be large, and a small stepsize will be needed for stability. See Roberts and Tweedie (1996) for a discussion of this in the context of the Langevin method (see Section 5.5.2).

This problem can be alleviated by choosing ε randomly from some distribution. Even if the mean of this distribution is too large, suitably small values for ε may be chosen occasionally. (See Section 5.3.2 for another reason to randomly vary the stepsize.) The random choice of ε should be done once at the start of a trajectory, not for every leapfrog step, since even if

all the choices are below the stability limit, random changes at each step lead to a random walk in the error for H, rather than the bounded error that is illustrated in Figure 5.3.

The "short-cut" procedures described in Section 5.5.6 can be seen as ways of saving computation time when a randomly chosen stepsize is inappropriate.

5.4.2.3 What Trajectory Length?

Choosing a suitable trajectory length is crucial if HMC is to explore the state space systematically, rather than by a random walk. Many distributions are difficult to sample from because they are tightly constrained in some directions, but much less constrained in other directions. Exploring the less constrained directions is best done using trajectories that are long enough to reach a point that is far from the current point in that direction. Trajectories can be too long, however, as is illustrated in Figure 5.3. The trajectory shown on the left of that figure is a bit too long, since it reverses direction and then ends at a point that might have been reached with a trajectory about half its length. If the trajectory were a little longer, the result could be even worse, since the trajectory would not only take longer to compute, but might also end near its starting point.

For more complex problems, one cannot expect to select a suitable trajectory length by looking at plots like Figure 5.3. Finding the linear combination of variables that is least confined will be difficult, and will be impossible when, as is typical, the least confined "direction" is actually a nonlinear curve or surface.

Setting the trajectory length by trial and error therefore seems necessary. For a problem thought to be fairly difficult, a trajectory with $L = 100$ might be a suitable starting point. If preliminary runs (with a suitable ε; see above) show that HMC reaches a nearly independent point after only one iteration, a smaller value of L might be tried next. (Unless these "preliminary" runs are actually sufficient, in which case there is of course no need to do more runs.) If instead there is high autocorrelation in the run with $L = 100$, runs with $L = 1000$ might be tried next.

As discussed at the end of Sections 5.3.2 and 5.3.3, randomly varying the length of the trajectory (over a fairly small interval) may be desirable, to avoid choosing a trajectory length that happens to produce a near-periodicity for some variable or combination of variables.

5.4.2.4 Using Multiple Stepsizes

Using the results in Section 5.4.1, we can exploit information about the relative scales of variables to improve the performance of HMC. This can be done in two equivalent ways. If s_i is a suitable scale for q_i, we could transform q, by setting $q_i' = q_i/s_i$, or we could instead use a kinetic energy function of $K(p) = p^T M^{-1} p$, with M being a diagonal matrix with diagonal elements $m_i = 1/s_i^2$.

A third equivalent way to exploit this information, which is often the most convenient, is to use different stepsizes for different pairs of position and momentum variables. To see how this works, consider a leapfrog update (following Equations 5.18 through 5.20) with $m_i = 1/s_i^2$:

$$
\begin{aligned}
p_i\,(t + \varepsilon/2) &= p_i(t) - (\varepsilon/2)\ \frac{\partial U}{\partial q_i}(q(t)), \\
q_i(t + \varepsilon) &= q_i(t) + \varepsilon\, s_i^2\, p_i\,(t + \varepsilon/2)\,, \\
p_i(t + \varepsilon) &= p_i\,(t + \varepsilon/2) - (\varepsilon/2)\ \frac{\partial U}{\partial q_i}(q(t + \varepsilon)).
\end{aligned}
$$

Define $(q^{(0)}, p^{(0)})$ to be the state at the beginning of the leapfrog step (i.e. $(q(t), p(t))$), define $(q^{(1)}, p^{(1)})$ to be the final state (i.e. $(q(t+\varepsilon), p(t+\varepsilon))$), and define $p^{(1/2)}$ to be half-way momentum (i.e. $p(t+\varepsilon/2)$). We can now rewrite the leapfrog step above as

$$\begin{aligned} p_i^{(1/2)} &= p_i^{(0)} - (\varepsilon/2)\,\frac{\partial U}{\partial q_i}(q^{(0)}), \\ q_i^{(1)} &= q_i^{(0)} + \varepsilon\, s_i^2\, p_i^{(1/2)}, \\ p_i^{(1)} &= p_i^{(1/2)} - (\varepsilon/2)\,\frac{\partial U}{\partial q_i}(q^{(1)}). \end{aligned}$$

If we now define rescaled momentum variables, $\tilde{p}_i = s_i p_i$, and stepsizes $\varepsilon_i = s_i \varepsilon$, we can write the leapfrog update as

$$\begin{aligned} \tilde{p}_i^{(1/2)} &= \tilde{p}_i^{(0)} - (\varepsilon_i/2)\,\frac{\partial U}{\partial q_i}(q^{(0)}), \\ q_i^{(1)} &= q_i^{(0)} + \varepsilon_i\, \tilde{p}_i^{(1/2)}, \\ \tilde{p}_i^{(1)} &= \tilde{p}_i^{(1/2)} - (\varepsilon_i/2)\,\frac{\partial U}{\partial q_i}(q^{(1)}). \end{aligned}$$

This is just like a leapfrog update with all $m_i = 1$, but with different stepsizes for different (q_i, p_i) pairs. Of course, the successive values for $(q, \tilde{p})$ can no longer be interpreted as following Hamiltonian dynamics at consistent time points, but that is of no consequence for the use of these trajectories in HMC. Note that when we sample for the momentum before each trajectory, each $\tilde{p}_i$ is drawn independently from a Gaussian distribution with mean zero and variance one, regardless of the value of s_i.

This multiple stepsize approach is often more convenient, especially when the estimated scales, s_i, are not fixed, as discussed in Section 5.4.5, and the momentum is only partially refreshed (Section 5.5.3).

5.4.3 Combining HMC with Other MCMC Updates

For some problems, MCMC using HMC alone will be impossible or undesirable. Two situations where non-HMC updates will be necessary are when some of the variables are discrete, and when the derivatives of the log probability density with respect to some of the variables are expensive or impossible to compute. HMC can then be feasibly applied only to the other variables. Another example is when special MCMC updates have been devised that may help convergence in ways that HMC does not—for example, by moving between otherwise isolated modes—but which are not a complete replacement for HMC. As discussed in Section 5.4.5 below, Bayesian hierarchical models may also be best handled with a combination of HMC and other methods such as Gibbs sampling.

In such circumstances, one or more HMC updates for all or a subset of the variables can be alternated with one or more other updates that leave the desired joint distribution of all variables invariant. The HMC updates can be viewed as either leaving this same joint distribution invariant, or as leaving invariant the conditional distribution of the variables that HMC changes, given the current values of the variables that are fixed during the HMC update. These are equivalent views, since the joint density can be factored as this conditional density times the marginal density of the variables that are fixed, which is just a constant

from the point of view of a single HMC update, and hence can be left out of the potential energy function.

When both HMC and other updates are used, it may be best to use shorter trajectories for HMC than would be used if only HMC were being done. This allows the other updates to be done more often, which presumably helps sampling. Finding the optimal tradeoff is likely to be difficult, however. A variation on HMC that reduces the need for such a tradeoff is described below in Section 5.5.3.

5.4.4 Scaling with Dimensionality

In Section 5.3.3, one of the main benefits of HMC was illustrated—its ability to avoid the inefficient exploration of the state space via a random walk. This benefit is present (to at least some degree) for most practical problems. For problems in which the dimensionality is moderate to high, another benefit of HMC over simple random-walk Metropolis methods is a slower increase in the computation time needed (for a given level of accuracy) as the dimensionality increases. (Note that here I will consider only sampling performance after equilibrium is reached, not the time needed to approach equilibrium from some initial state not typical of the distribution, which is harder to analyze.)

5.4.4.1 Creating Distributions of Increasing Dimensionality by Replication

To talk about how performance scales with dimensionality we need to assume something about how the distribution changes with dimensionality, d.

I will assume that dimensionality increases by adding independent replicas of variables—that is, the potential energy function for $q = (q_1, \ldots, q_d)$ has the form $U(q) = \Sigma\, u_i(q_i)$, for functions u_i drawn independently from some distribution. Of course, this is not what any real practical problem is like, but it may be a reasonable model of the effect of increasing dimensionality for some problems—for instance, in statistical physics, distant regions of large systems are often nearly independent. Note that the independence assumption itself is not crucial since, as discussed in Section 5.4.1, the performance of HMC (and of simple random-walk Metropolis) does not change if independence is removed by rotating the coordinate system, provided the kinetic energy function (or random-walk proposal distribution) is rotationally symmetric.

For distributions of this form, in which the variables are independent, Gibbs sampling will perform very well (assuming it is feasible), producing an independent point after each scan of all variables. Applying Metropolis updates to each variable separately will also work well, provided the time for a single-variable update does not grow with d. However, these methods are not invariant to rotation, so this good performance may not generalize to the more interesting distributions for which we hope to obtain insight with the analysis below.

5.4.4.2 Scaling of HMC and Random-Walk Metropolis

Here, I discuss informally how well HMC and random-walk Metropolis scale with dimension, loosely following Creutz (1988, Section III).

To begin, Cruetz notes that the following relationship holds when any Metropolis-style algorithm is used to sample a density $P(x) = (1/Z)\exp(-E(x))$:

$$1 = \mathrm{E}\,[P(x^*)/P(x)] = \mathrm{E}\,[\exp(-(E(x^*) - E(x)))] = \mathrm{E}\,[\exp(-\Delta)], \tag{5.26}$$

where x is the current state, assumed to be distributed according to $P(x)$, x^* is the proposed state, and $\Delta = E(x^*) - E(x)$. Jensen's inequality then implies that the expectation of the energy difference is nonnegative:

$$\mathrm{E}[\Delta] \geq 0.$$

The inequality will usually be strict.

When $U(q) = \Sigma\, u_i(q_i)$, and proposals are produced independently for each i, we can apply these relationships either to a single variable (or pair of variables) or to the entire state. For a single variable (or pair), I will write Δ_1 for $E(x^*) - E(x)$, with $x = q_i$ and $E(x) = u_i(q_i)$, or $x = (q_i, p_i)$ and $E(x) = u_i(q_i) + p_i^2/2$. For the entire state, I will write Δ_d for $E(x^*) - E(x)$, with $x = q$ and $E(x) = U(q)$, or $x = (q, p)$ and $E(x) = U(q) + K(p)$. For both random-walk Metropolis and HMC, increasing dimension by replicating variables will lead to increasing energy differences, since Δ_d is the sum of Δ_1 for each variable, each of which has positive mean. This will lead to a decrease in the acceptance probability—equal to $\min(1, \exp(-\Delta_d))$—unless the width of the proposal distribution or the leapfrog stepsize is decreased to compensate.

More specifically, for random-walk Metropolis with proposals that change each variable independently, the difference in potential energy between a proposed state and the current state will be the sum of independent differences for each variable. If we fix the standard deviation, ς, for each proposed change, the mean and the variance of this potential energy difference will both grow linearly with d, which will lead to a progressively lower acceptance rate. To maintain reasonable performance, ς will have to decrease as d increases. Furthermore, the number of iterations needed to reach a nearly independent point will be proportional to ς^{-2}, since exploration is via a random walk.

Similarly, when HMC is used to sample from a distribution in which the components of q are independent, using the kinetic energy $K(p) = \Sigma\, p_i^2/2$, the different (q_i, p_i) pairs do not interact during the simulation of a trajectory—each (q_i, p_i) pair follows Hamiltonian dynamics according to just the one term in the potential energy involving q_i and the one term in the kinetic energy involving p_i. There is therefore no need for the length in fictitious time of a trajectory to increase with dimensionality. However, acceptance of the endpoint of the trajectory is based on the error in H due to the leapfrog approximation, which is the sum of the errors pertaining to each (q_i, p_i) pair. For a fixed stepsize, ε, and fixed trajectory length, εL, both the mean and the variance of the error in H grow linearly with d. This will lead to a progressively lower acceptance rate as dimensionality increases, if it is not counteracted by a decrease in ε. The number of leapfrog steps needed to reach an independent point will be proportional to ε^{-1}.

To see which method scales better, we need to determine how rapidly we must reduce ς and ε as d increases, in order to maintain a reasonable acceptance rate. As d increases and ς or ε goes to zero, Δ_1 will go to zero as well. Using a second-order approximation of $\exp(-\Delta_1)$ as $1 - \Delta_1 + \Delta_1^2/2$, together with Equation 5.26, we find that

$$\mathrm{E}[\Delta_1] \approx \frac{\mathrm{E}[\Delta_1^2]}{2}. \tag{5.27}$$

It follows from this that the variance of Δ_1 is twice the mean of Δ_1 (when Δ_1 is small), which implies that the variance of Δ_d is twice the mean of Δ_d (even when Δ_d is not small). To achieve a good acceptance rate, we must therefore keep the mean of Δ_d near one, since a large mean will not be saved by a similarly large standard deviation (which would produce fairly frequent acceptances as Δ_d occasionally takes on a negative value).

For random-walk Metropolis with a symmetric proposal distribution, we can see how ς needs to scale by directly averaging Δ_1 for a proposal and its inverse. Let the proposal for

one variable be $x^* = x + c$, and suppose that $c = a$ and $c = -a$ are equally likely. Approximating $U(x^*)$ to second order as $U(x) + cU'(x) + c^2U''(x)/2$, we find that the average of $\Delta_1 = U(x^*) - U(x)$ over $c = a$ and $c = -a$ is $a^2U''(x)$. Averaging this over the distribution of a, with standard deviation ς, and over the distribution of x, we see that $\mathrm{E}[\Delta_1]$ is proportional to ς^2. It follows that $\mathrm{E}[\Delta_d]$ is proportional to $d\varsigma^2$, so we can maintain a reasonable acceptance rate by letting ς be proportional to $d^{-1/2}$. The number of iterations needed to reach a nearly independent point will be proportional to ς^{-2}, which will be proportional to d. The amount of computation time needed will typically be proportional to d^2.

As discussed at the end of Section 5.2.3, the error in H when using the leapfrog discretization to simulate a trajectory of a fixed length is proportional to ε^2 (for sufficiently small ε). The error in H for a single (q_i, p_i) pair is the same as Δ_1, so we see that Δ_1^2 is proportional to ε^4. Equation 5.27 then implies that $\mathrm{E}[\Delta_1]$ is also proportional to ε^4. The average total error in H for all variables, $\mathrm{E}[\Delta_d]$, will be proportional to $d\varepsilon^4$, and hence we must make ε be proportional to $d^{-1/4}$ to maintain a reasonable acceptance rate. The number of leapfrog updates to reach a nearly independent point will therefore grow as $d^{1/4}$, and the amount of computation time will typically grow as $d^{5/4}$, which is much better than the d^2 growth for random-walk Metropolis.

5.4.4.3 Optimal Acceptance Rates

By extending the analysis above, we can determine what the acceptance rate of proposals is when the optimal choice of ς or ϵ is used. This is helpful when tuning the algorithms—provided, of course, that the distribution sampled is high-dimensional, and has properties that are adequately modeled by a distribution with replicated variables.

To find this acceptance rate, we first note that since Metropolis methods satisfy detailed balance, the probability of an accepted proposal with Δ_d negative must be equal to the probability of an accepted proposal with Δ_d positive. Since all proposals with negative Δ_d are accepted, the acceptance rate is simply twice the probability that a proposal has a negative Δ_d. For large d, the central limit theorem implies that the distribution of Δ_d is Gaussian, since it is a sum of d independent Δ_1 values. (This assumes that the variance of each Δ_1 is finite.) We saw above that the variance of Δ_d is twice its mean, $\mathrm{E}[\Delta_d] = \mu$. The acceptance probability can therefore be written as follows (Gupta et al., 1990), for large d:

$$P(\text{accept}) = 2\,\Phi\left(\frac{(0-\mu)}{\sqrt{2\mu}}\right) = 2\,\Phi\left(-\sqrt{\mu/2}\right) = a(\mu), \tag{5.28}$$

where $\Phi(z)$ is the cumulative distribution function for a Gaussian variable with mean zero and variance one.

For random-walk Metropolis, the cost of obtaining an independent point will be proportional to $1/(a\varsigma^2)$, where a is the acceptance rate. We saw above that $\mu = \mathrm{E}[\Delta_d]$ is proportional to ς^2, so the cost follows the proportionality

$$C_{\mathrm{rw}} \propto \frac{1}{(a(\mu)\mu)}.$$

Numerical calculation shows that this is minimized when $\mu = 2.8$ and $a(\mu) = 0.23$.

For HMC, the cost of obtaining an independent point will be proportional to $1/(a\varepsilon)$, and as we saw above, μ is proportional to ε^4. From this we obtain

$$C_{\text{HMC}} \propto \frac{1}{(a(\mu)\mu^{1/4})}.$$

Numerical calculation shows that the minimum is when $\mu = 0.41$ and $a(\mu) = 0.65$.

The same optimal 23% acceptance rate for random-walk Metropolis was previously obtained using a more formal analysis by Roberts et al. (1997). The optimal 65% acceptance rate for HMC that I derive above is consistent with previous empirical results on distributions following the model here (Neal, 1994, Figure 2), and on real high-dimensional problems (Creutz, 1988, Figures 2 and 3; Sexton and Weingarten, 1992, Table 1). Kennedy and Pendleton (1991) obtained explicit and rigorous results for HMC applied to multivariate Gaussian distributions.

5.4.4.4 Exploring the Distribution of Potential Energy

The better scaling behavior of HMC seen above depends crucially on the resampling of momentum variables. We can see this by considering how well the methods explore the distribution of the potential energy, $U(q) = \Sigma\, u_i(q_i)$. Because $U(q)$ is a sum of d independent terms, its standard deviation will grow in proportion to $d^{1/2}$.

Following Caracciolo et al. (1994), we note that the expected change in potential energy from a single Metropolis update will be no more than order 1—intuitively, large upwards changes are unlikely to be accepted, and since Metropolis updates satisfy detailed balance, large downward changes must also be rare (in equilibrium). Because changes in U will follow a random walk (due again to detailed balance), it will take at least order $(d^{1/2}/\,1)^2 = d$ Metropolis updates to explore the distribution of U.

In the first step of an HMC iteration, the resampling of momentum variables will typically change the kinetic energy by an amount that is proportional to $d^{1/2}$, since the kinetic energy is also a sum of d independent terms, and hence has standard deviation that grows as $d^{1/2}$ (more precisely, its standard deviation is $d^{1/2}/2^{1/2}$). If the second step of HMC proposes a distant point, this change in kinetic energy (and hence in H) will tend, by the end of the trajectory, to have become equally split between kinetic and potential energy. If the endpoint of this trajectory is accepted, the change in potential energy from a single HMC iteration will be proportional to $d^{1/2}$, comparable to its overall range of variation. So, in contrast to random-walk Metropolis, we may hope that only a few HMC iterations will be sufficient to move to a nearly independent point, even for high-dimensional distributions.

Analyzing how well methods explore the distribution of U can also provide insight into their performance on distributions that are not well modeled by replication of variables, as we will see in the next section.

5.4.5 HMC for Hierarchical Models

Many Bayesian models are defined hierarchically. A large set of low-level parameters have prior distributions that are determined by fewer higher-level "hyperparameters," which in turn may have priors determined by yet-higher-level hyperparameters. For example, in a regression model with many predictor variables, the regression coefficients might be given Gaussian prior distributions, with a mean of zero and a variance that is a hyperparameter. This hyperparameter could be given a broad prior distribution, so that its posterior distribution is determined mostly by the data.

One could apply HMC to these models in an obvious way (after taking the logs of variance hyperparameters, so they will be unconstrained). However, it may be better to apply HMC only to the lower-level parameters, for reasons I will now discuss. (See Section 5.4.3 for general discussion of applying HMC to a subset of variables.)

I will use my work on Bayesian neural network models (Neal, 1996a) as an example. Such models typically have several groups of low-level parameters, each with an associated variance hyperparameter. The posterior distribution of these hyperparameters reflects important aspects of the data, such as which predictor variables are most relevant to the task. The efficiency with which values for these hyperparameters are sampled from the posterior distribution can often determine the overall efficiency of the MCMC method.

I use HMC only for the low-level parameters in Bayesian neural network models, with the hyperparameters being fixed during an HMC update. These HMC updates alternate with Gibbs sampling updates of the hyperparameters, which (in the simpler versions of the models) are independent given the low-level parameters, and have conditional distributions of standard form. By using HMC only for the low-level parameters, the leapfrog stepsizes used can be set using heuristics that are based on the current hyperparameter values. (I use the multiple stepsize approach described at the end of Section 5.4.2, equivalent to using different mass values, m_i, for different parameters.) For example, the size of the network "weights" on connections out of a "hidden unit" determine how sensitive the likelihood function is to changes in weights on connections into the hidden unit; the variance of the weights on these outgoing connections is therefore useful in setting the stepsize for the weights on the incoming connections. If the hyperparameters were changed by the same HMC updates as change the lower-level parameters, using them to set stepsizes would not be valid, since a reversed trajectory would use different stepsizes, and hence not retrace the original trajectory. Without a good way to set stepsizes, HMC for the low-level parameters would likely be much less efficient.

Choo (2000) bypassed this problem by using a modification of HMC in which trajectories are simulated by alternating leapfrog steps that update only the hyperparameters with leapfrog steps that update only the low-level parameters. This procedure maintains both reversibility and volume-preservation (though not necessarily symplecticness), while allowing the stepsizes for the low-level parameters to be set using the current values of the hyperparameters (and vice versa). However, performance did not improve as hoped because of a second issue with hierarchical models.

In these Bayesian neural network models, and many other hierarchical models, the joint distribution of both low-level parameters and hyperparameters is highly skewed, with the probability density varying hugely from one region of high posterior probability to another. Unless the hyperparameters controlling the variances of low-level parameters have very narrow posterior distributions, the joint posterior density for hyperparameters and low-level parameters will vary greatly from when the variance is low to when it is high.

For instance, suppose that in its region of high posterior probability, a variance hyperparameter varies by a factor of 4. If this hyperparameter controls 1000 low-level parameters, their typical prior probability density will vary by a factor of $2^{1000} = 1.07 \times 10^{301}$, corresponding to a potential energy range of $\log(2^{1000}) = 693$, with a standard deviation of $693/12^{1/2} = 200$ (since the variance of a uniform distribution is one twelfth of its range). As discussed at the end of Section 5.4.4, one HMC iteration changes the energy only through the resampling of the momentum variables, which at best leads to a change in potential energy with standard deviation of about $d^{1/2}/2^{3/2}$. For this example, with 1000 low-level

parameters, this is 11.2, so about $(200/11.2)^2 = 319$ HMC iterations will be needed to reach an independent point.

One might obtain similar performance for this example using Gibbs sampling. However, for neural network models, there is no feasible way of using Gibbs sampling for the posterior distribution of the low-level parameters, but HMC can be applied to the conditional distribution of the low-level parameters given the hyperparameters. Gibbs sampling can then be used to update the hyperparameters. As we have seen, performance would not be improved by trying to update the hyperparameters with HMC as well, and updating them by Gibbs sampling is easier.

Choo (2000) tried another approach that could potentially improve on this—reparameterizing low-level parameters θ_i, all with variance $\exp(\kappa)$, by letting $\theta_i = \phi_i \exp(\kappa/2)$, and then sampling for κ and the ϕ_i using HMC. The reparameterization eliminates the extreme variation in probability density that HMC cannot efficiently sample. However, he found that it is difficult to set a suitable stepsize for κ, and that the error in H tended to grow with trajectory length, unlike the typical situation when HMC is used only for the low-level parameters. Use of "tempering" techniques (see Section 5.5.7) is another possibility.

Even though it does not eliminate all difficulties, HMC is very useful for Bayesian neural network models—indeed, without it, they might not be feasible for most applications. Using HMC for at least the low-level parameter can produce similar benefits for other hierarchical models (e.g. Ishwaran, 1999), especially when the posterior correlations of these low-level parameters are high. As in any application of HMC, however, careful tuning of the stepsize and trajectory length is generally necessary.

5.5 Extensions of and Variations on HMC

The basic HMC algorithm (Figure 5.2) can be modified in many ways, either to improve its efficiency, or to make it useful for a wider range of distributions. In this section, I will start by discussing alternatives to the leapfrog discretization of Hamilton's equations, and also show how HMC can handle distributions with constraints on the variables (e.g. variables that must be positive). I will then discuss a special case of HMC—when only one leapfrog step is done—and show how it can be extended to produce an alternative method of avoiding random walks, which may be useful when not all variables are updated by HMC. Most applications of HMC can benefit from using a variant in which "windows" of states are used to increase the acceptance probability. Another widely applicable technique is to use approximations to the Hamiltonian to compute trajectories, while still obtaining correct results by using the exact Hamiltonian when deciding whether to accept the endpoint of the trajectory. Tuning of HMC may be assisted by using a "short-cut" method that avoids computing the whole trajectory when the stepsize is inappropriate. Tempering methods have potential to help with distributions having multiple modes, or which are highly skewed.

There are many other variations that I will not be able to review here, such as the use of a "shadow Hamiltonian" that is exactly conserved by the inexact simulation of the real Hamiltonian (Izagguirre and Hampton, 2004), and the use of symplectic integration methods more sophisticated than the leapfrog method (e.g. Creutz and Gocksch, 1989), including a recent proposal by Girolami et al. (2009) to use a symplectic integrator for a nonseparable

Hamiltonian in which M in the kinetic energy of (Equation 5.5) depends on q, allowing for "adaptation" based on local information.

5.5.1 Discretization by Splitting: Handling Constraints and Other Applications

The leapfrog method is not the only discretization of Hamilton's equations that is reversible and volume-preserving, and hence can be used for HMC. Many "symplectic integration methods" have been devised, mostly for applications other than HMC (e.g. simulating the solar system for millions of years to test its stability). It is possible to devise methods that have a higher order of accuracy than the leapfrog method (see, e.g. McLachlan and Atela, 1992). Using such a method for HMC will produce asymptotically better performance than the leapfrog method, as dimensionality increases. Experience has shown, however, that the leapfrog method is hard to beat in practice.

Nevertheless, it is worth taking a more general look at how Hamiltonian dynamics can be simulated, since this also points to how constraints on the variables can be handled, as well as possible improvements such as exploiting partial analytic solutions.

5.5.1.1 Splitting the Hamiltonian

Many symplectic discretizations of Hamiltonian dynamics can be derived by "splitting" the Hamiltonian into several terms, and then, for each term in succession, simulating the dynamics defined by that term for some small time step, then repeating this procedure until the desired total simulation time is reached. If the simulation for each term can be done analytically, we obtain a symplectic approximation to the dynamics that is feasible to implement.

This general scheme is described by Leimkuhler and Reich (2004, Section 4.2) and by Sexton and Weingarten (1992). Suppose that the Hamiltonian can be written as a sum of k terms, as follows:

$$H(q,p) = H_1(q,p) + H_2(q,p) + \cdots + H_{k-1}(q,p) + H_k(q,p).$$

Suppose also that we can *exactly* implement Hamiltonian dynamics based on each H_i, for $i = 1, \ldots, k$, with $T_{i,\varepsilon}$ being the mapping defined by applying dynamics based on H_i for time ε. As shown by Leimkuhler and Reich, if the H_i are twice differentiable, the composition of these mappings, $T_{1,\varepsilon} \circ T_{2,\varepsilon} \circ \cdots \circ T_{k-1,\varepsilon} \circ T_{k,\varepsilon}$, is a valid discretization of Hamiltonian dynamics based on H, which will reproduce the exact dynamics in the limit as ε goes to zero, with global error of order ε or less.

Furthermore, this discretization will preserve volume, and will be symplectic, since these properties are satisfied by each of the $T_{i,\varepsilon}$ mappings. The discretization will also be reversible if the sequence of H_i is symmetrical—that is, $H_i(q,p) = H_{k-i+1}(q,p)$. As mentioned at the end of Section 5.2.3, any reversible method must have global error of even order in ε (Leimkuhler and Reich, 2004, Section 4.3.3), which means that the global error must be of order ε^2 or better.

We can derive the leapfrog method from a symmetrical splitting of the Hamiltonian. If $H(q,p) = U(q) + K(p)$, we can write the Hamiltonian as

$$H(q,p) = \frac{U(q)}{2} + K(p) + \frac{U(q)}{2},$$

which corresponds to a split with $H_1(q,p) = H_3(q,p) = U(q)/2$ and $H_2(q,p) = K(p)$. Hamiltonian dynamics based on H_1 is (Equations 5.1 and 5.2):

$$\frac{dq_i}{dt} = \frac{\partial H_1}{\partial p_i} = 0,$$
$$\frac{dp_i}{dt} = -\frac{\partial H_1}{\partial q_i} = -\frac{1}{2}\frac{\partial U}{\partial q_i}.$$

Applying this dynamics for time ε just adds $-(\varepsilon/2)\,\partial U/\partial q_i$ to each p_i, which is the first part of a leapfrog step (Equation 5.18). The dynamics based on H_2 is as follows:

$$\frac{dq_i}{dt} = \frac{\partial H_2}{\partial p_i} = \frac{\partial K}{\partial p_i},$$
$$\frac{dp_i}{dt} = -\frac{\partial H_2}{\partial q_i} = 0.$$

If $K(p) = \frac{1}{2}\sum p_i^2/m_i$, applying this dynamics for time ϵ results in adding $\varepsilon p_i/m_i$ to each q_i, which is the second part of a leapfrog step Equation 5.19. Finally, H_3 produces the third part of a leapfrog step (Equation 5.20), which is the same as the first part, since $H_3 = H_1$.

5.5.1.2 Splitting to Exploit Partial Analytical Solutions

One situation where splitting can help is when the potential energy contains a term that can, on its own, be handled analytically. For example, the potential energy for a Bayesian posterior distribution will be the sum of minus the log prior density for the parameters and minus the log likelihood. If the prior is Gaussian, the log prior density term will be quadratic, and can be handled analytically (see the one-dimensional example at the end of Section 5.2.1).

We can modify the leapfrog method for this situation by using a modified split. Suppose that $U(q) = U_0(q) + U_1(q)$, with U_0 being analytically tractable, in conjunction with the kinetic energy, $K(p)$. We use the split

$$H(q,p) = \frac{U_1(q)}{2} + \big[U_0(q) + K(p)\big] + \frac{U_1(q)}{2}, \tag{5.29}$$

that is, $H_1(q,p) = H_3(q,p) = U_1(q)/2$ and $H_2(q,p) = U_0(q) + K(p)$. The first and last half steps for p are the same as for ordinary leapfrog, based on U_1 alone. The middle full step for q, which in ordinary leapfrog just adds εp to q, is replaced by the analytical solution for following the exact dynamics based on the Hamiltonian $U_0(q) + K(p)$ for time ε.

With this procedure, it should be possible to use a larger stepsize (and hence use fewer steps in a trajectory), since part of the potential energy has been separated out and handled exactly. The benefit of handling the prior exactly may be limited, however, since the prior is usually dominated by the likelihood.

5.5.1.3 Splitting Potential Energies with Variable Computation Costs

Splitting can also help if the potential energy function can be split into two terms, one of which requires less computation time to evaluate than the other (Sexton and Weingarten,

1992). Suppose that $U(q) = U_0(q) + U_1(q)$, with U_0 being cheaper to compute than U_1, and let the kinetic energy be $K(p)$. We can use the following split, for some $M > 1$:

$$H(q,p) = \frac{U_1(q)}{2} + \sum_{m=1}^{M} \left[\frac{U_0(q)}{2M} + \frac{K(p)}{M} + \frac{U_0(q)}{2M} \right] + \frac{U_1(q)}{2}.$$

We label the $k = 3M + 2$ terms as $H_1(q,p) = H_k(q,p) = U_1(q)/2$ and, for $i = 1, \ldots, M$, $H_{3i-1}(q,p) = H_{3i+1}(q,p) = U_0(q)/2M$ and $H_{3i}(q,p) = K(p)/M$. The resulting discretization can be seen as a nested leapfrog method. The M inner leapfrog steps involve only U_0, and use an effective stepsize of ε/M. The outer leapfrog step takes half steps for p using only U_1, and replaces the update for q in the middle with the M inner leapfrog steps.

If U_0 is much cheaper to compute than U_1, we can use a large value for M without increasing computation time by much. The stepsize, ε, that we can use will then be limited mostly by the properties of U_1, since the effective stepsize for U_0 is much smaller, ε/M. Using a bigger ε than with the standard leapfrog method will usually be possible, and hence we will need fewer steps in a trajectory, with fewer computations of U_1.

5.5.1.4 Splitting according to Data Subsets

When sampling from the posterior distribution for a Bayesian model of independent data points, it may be possible to save computation time by splitting the potential energy into terms for subsets of the data.

Suppose that we partition the data into subsets S_m, for $m = 1, \ldots, M$, typically of roughly equal size. We can then write the log likelihood function as $\ell(q) = \sum_{m=1}^{M} \ell_m(q)$, where ℓ_m is the log likelihood function based on the data points in S_m. If $\pi(q)$ is the prior density for the parameters, we can let $U_m(q) = -\log(\pi(q))/M - \ell_m(q)$, and split the Hamiltonian as follows:

$$H(q,p) = \sum_{m=1}^{M} \left[\frac{U_m(q)}{2} + K(p) \Big/ M + \frac{U_m(q)}{2} \right];$$

that is, we let the $k = 3M$ terms be $H_{3m-2}(q,p) = H_{3m}(q,p) = U_m(q)/2$ and $H_{3m-1}(q,p) = K(p)/m$. The resulting discretization with stepsize ε effectively performs M leapfrog steps with stepsize ε/M, with the mth step using MU_m as the potential energy function.

This scheme can be beneficial if the data set is redundant, with many data points that are similar. We then expect $MU_m(q)$ to be approximately the same as $U(q)$, and we might hope that we could set ε to be M times larger than with the standard leapfrog method, obtaining similar results with M times less computation. In practice, however, the error in H at the end of the trajectory will be larger than with standard leapfrog, so the gain will be less than this. I found (Neal, 1996a, Sections 3.5.1 and 3.5.2) that the method can be beneficial for neural network models, especially when combined with the windowed HMC procedure described below in Section 5.5.4.

Note that unlike the other examples above, this split is *not* symmetrical, and hence the resulting discretization is not reversible. However, it can still be used to produce a proposal for HMC as long as the labeling of the subsets is randomized for each iteration, so that the reverse trajectory has the same probability of being produced as the forward trajectory. (It is possible, however, that some symmetrical variation on this split might produce better results.)

5.5.1.5 Handling Constraints

An argument based on splitting shows how to handle constraints on the variables being sampled. Here, I will consider only separate constraints on some subset of the variables, with the constraint on q_i taking the form $q_i \le u_i$, or $q_i \ge l_i$, or both. A similar scheme can handle constraints taking the form $G(q) \ge 0$, for any differentiable function G.

We can impose constraints on variables by letting the potential energy be infinite for values of q that violate any of the constraints, which will give such points probability zero. To see how to handle such infinite potential energies, we can look at a limit of potential energy functions that approach infinity, and the corresponding limit of the dynamics.

To illustrate, suppose that $U_*(q)$ is the potential energy ignoring constraints, and that q_i is constrained to be less than u_i. We can take the limit as $r \to \infty$ of the following potential energy function (which is one of many that could be used):

$$U(q) = U_*(q) + C_r(q_i, u_i), \quad \text{where } C_r(q_i, u_i) = \begin{cases} 0, & \text{if } q_i \le u_i, \\ r^{r+1}(q_i - u_i)^r, & \text{if } q_i > u_i. \end{cases}$$

It is easy to see that $\lim_{r\to\infty} C_r(q_i, u_i)$ is zero for any $q_i \le u_i$ and infinity for any $q_i > u_i$. For any finite $r > 1$, $U(q)$ is differentiable, so we can use it to define Hamiltonian dynamics.

To simulate the dynamics based on this $U(q)$, with a kinetic energy $K(p) = \frac{1}{2}\sum p_i^2/m_i$, we can use the split of Equation 5.29, with $U_1(q) = U_*(q)$ and $U_0(q) = C_r(q_i, u_i)$:

$$H(q,p) = \frac{U_*(q)}{2} + \big[C_r(q_i, u_i) + K(p)\big] + \frac{U_*(q)}{2}.$$

This produces a variation on the leapfrog method in which the half steps for p (Equations 5.18 and 5.19) remain the same, but the full step for q (Equation 5.19) is modified to account for the constraint on q_i. After computing $q_i' = q_i(t) + \varepsilon p_i(t + \varepsilon/2)/m_i$, we check if $q_i' > u_i$. If not, the value of $C_r(q_i, u_i)$ must be zero all along the path from q_i to q_i', and we can set $q(t + \varepsilon)$ to q_i'. But if $q_i' > u_i$, the dynamics based on the Hamiltonian $C_r(q_i, u_i) + K(p)$ will be affected by the C_r term. This term can be seen as a steep hill, which will be climbed as q_i moves past u_i, until the point is reached where C_r is equal to the previous value of $\frac{1}{2}p_i^2/m_i$, at which point p_i will be zero. (If r is sufficiently large, as it will be in the limit as $r \to \infty$, this point will be reached before the end of the full step.) We will then fall down the hill, with p_i taking on increasingly negative values, until we again reach $q_i = u_i$, when p_i will be just the negative of the original value of p_i. We then continue, now moving in the opposite direction, away from the upper limit.

If several variables have constraints, we must follow this procedure for each, and if a variable has both upper and lower constraints, we must repeat the procedure until neither constraint is violated. The end result is that the full step for q of Equation 5.19 is replaced by the procedure shown in Figure 5.8. Intuitively, the trajectory just bounces off the "walls" given by the constraints. If $U_*(q)$ is constant, these bounces are the only interesting aspect of the dynamics, and the procedure is sometimes referred to as "billiards" (see, e.g. Ruján, 1997).

5.5.2 Taking One Step at a Time—The Langevin Method

A special case of HMC arises when the trajectory used to propose a new state consists of only a single leapfrog step. Suppose that we use the kinetic energy $K(p) = \frac{1}{2}\sum p_i^2$. An

```
For each variable, i=1,...,d:

  1) Let p'_i = p_i(t+ε/2)
  2) Let q'_i=q_i(t)+εp'_i/m_i
  3) If q_i is constrained, repeat the following until q'_i satisfies
     all constraints:
      a)  If q_i has an upper constraint, and q'_i > u_i
             Let q'_i=u_i-(q'_i-u_i) and p'_i=-p'_i
      b)  If q_i has a lower constraint, and q'_i < l_i
             Let q'_i=l_i+(l_i-q'_i) and p'_i=-p'_i
  4) Let q_i(t+ε)=q'_i and p_i(t+ε/2)=p'_i
```

FIGURE 5.8
Modification to the leapfrog update of q (Equation 5.19) to handle constraints of the form $q_i \le u_i$ or $q_i \le l_i$.

iteration of HMC with one leapfrog step can be expressed in the following way. We sample values for the momentum variables, p, from their Gaussian distributions with mean zero and variance one, and then propose new values, q^* and p^*, as follows:

$$q_i^* = q_i - \frac{\varepsilon^2}{2}\frac{\partial U}{\partial q_i}(q) + \varepsilon p_i, \tag{5.30}$$

$$p_i^* = p_i - \frac{\varepsilon}{2}\frac{\partial U}{\partial q_i}(q) - \frac{\varepsilon}{2}\frac{\partial U}{\partial q_i}(q^*). \tag{5.31}$$

We accept q^* as the new state with probability

$$\min\left[1,\ \exp\left(-(U(q^*) - U(q)) - \frac{1}{2}\sum_i((p_i^*)^2 - p_i^2)\right)\right], \tag{5.32}$$

and otherwise keep q as the new state. Equation 5.30 is known in physics as one type of "Langevin equation," and this method is therefore known as *Langevin Monte Carlo* (LMC) in the lattice field theory literature (e.g. Kennedy, 1990).

One can also remove any explicit mention of momentum variables, and view this method as performing a Metropolis–Hastings update in which q^* is proposed from a Gaussian distribution where the q_i^* are independent, with means of $q_i - (\varepsilon^2/2)[\partial U/\partial q_i](q)$ and variances of ε^2. Since this proposal is not symmetrical, it must be accepted or rejected based both on the ratio of the probability densities of q^* and q and on the ratio of the probability densities for proposing q from q^* and vice versa (Hastings, 1970). To see the equivalence with HMC using one leapfrog step, we can write the Metropolis–Hastings acceptance probability as follows:

$$\min\left[1,\ \frac{\exp(-U(q^*))}{\exp(-U(q))}\prod_{i=1}^{d}\frac{\exp\left(-\left(q_i - q_i^* + (\varepsilon^2/2)\,[\partial U/\partial q_i](q^*)\right)^2/2\varepsilon^2\right)}{\exp\left(-\left(q_i^* - q_i + (\varepsilon^2/2)\,[\partial U/\partial q_i](q)\right)^2/2\varepsilon^2\right)}\right]. \tag{5.33}$$

To see that this is the same as Equation 5.32, note that using Equations 5.30 and 5.31, we can write

$$p = \frac{1}{\varepsilon}\left[q_i^* - q_i + \frac{\varepsilon^2}{2}\frac{\partial U}{\partial q_i}(q)\right],$$

$$p^* = -\frac{1}{\varepsilon}\left[q_i - q_i^* + \frac{\varepsilon^2}{2}\frac{\partial U}{\partial q_i}(q^*)\right].$$

After substituting these into Equation 5.32, it is straightforward to see the equivalence to Equation 5.33.

In this Metropolis–Hastings form, the LMC method was first proposed by Rossky et al. (1978) for use in physical simulations. Approximate Langevin methods without an accept/reject step can also be used (for a discussion of this, see Neal, 1993, Section 5.3)—as, for instance, in a paper on statistical inference for complex models by Grenander and Miller (1990), where also an accept/reject step is proposed in the discussion by J. Besag (p. 591).

Although LMC can be seen as a special case of HMC, its properties are quite different. Since LMC updates are reversible, and generally make only small changes to the state (since ε typically cannot be very large), LMC will explore the distribution via an inefficient random walk, just like random-walk Metropolis updates.

However, LMC has better scaling behavior than random-walk Metropolis as dimensionality increases, as can be seen from an analysis paralleling that in Section 5.4.4 (Creutz, 1988; Kennedy, 1990). The local error of the leapfrog step is of order ε^3, so $\mathrm{E}[\Delta_1^2]$, the average squared error in H from one variable, will be of order ε^6. From Equation 5.27, $\mathrm{E}[\Delta]$ will also be of order ε^6, and with d independent variables, $\mathrm{E}[\Delta_d]$ will be of order $d\varepsilon^6$, so that ε must scale as $d^{-1/6}$ in order to maintain a reasonable acceptance rate. Since LMC explores the distribution via a random walk, the number of iterations needed to reach a nearly independent point will be proportional to ε^{-2}, which grows as $d^{1/3}$, and the computation time to reach a nearly independent point grows as $d^{4/3}$. This is better than the d^2 growth in computation time for random-walk Metropolis, but worse than the $d^{5/4}$ growth when HMC is used with trajectories that are long enough to reach a nearly independent point.

We can also find what the acceptance rate for LMC will be when the optimal ε is used, when sampling a distribution with independent variables replicated d times. As for random-walk Metropolis and HMC, the acceptance rate is given in terms of $\mu = \mathrm{E}[\Delta_d]$ by Equation 5.28. The cost of obtaining a nearly independent point using LMC is proportional to $1/(a(\mu)\varepsilon^2)$, and since μ is proportional to ε^6, we can write the cost as

$$C_{\mathrm{LMC}} \propto \frac{1}{(a(\mu)\mu^{1/3})}.$$

Numerical calculation shows that this is minimized when $a(\mu)$ is 0.57, a result obtained more formally by Roberts and Rosenthal (1998). This may be useful for tuning, if the behavior of LMC for the distribution being sampled resembles its behavior when sampling for replicated independent variables.

5.5.3 Partial Momentum Refreshment: Another Way to Avoid Random Walks

The single leapfrog step used in the LMC algorithm will usually not be sufficient to move to a nearly independent point, so LMC will explore the distribution via an inefficient random

walk. This is why HMC is typically used with trajectories of many leapfrog steps. An alternative that can suppress random-walk behavior even when trajectories consist of just one leapfrog step is to only partially refresh the momentum between trajectories, as proposed by Horowitz (1991).

Suppose that the kinetic energy has the typical form $K(p) = p^T M^{-1} p/2$. The following update for p will leave invariant the distribution for the momentum (Gaussian with mean zero and covariance M):

$$p' = \alpha p + (1 - \alpha^2)^{1/2} n. \tag{5.34}$$

Here, α is any constant in the interval $[-1, +1]$, and n is a Gaussian random vector with mean zero and covariance matrix M. To see this, note that if p has the required Gaussian distribution, the distribution of p' will also be Gaussian (since it is a linear combination of independent Gaussians), with mean 0 and covariance $\alpha^2 M + (1 - \alpha^2)M = M$.

If α is only slightly less than one, p' will be similar to p, but repeated updates of this sort will eventually produce a value for the momentum variables almost independent of the initial value. When $\alpha = 0$, p' is just set to a random value drawn from its Gaussian distribution, independent of its previous value. Note that when M is diagonal, the update of each momentum variable, p_i, is independent of the updates of other momentum variables.

The partial momentum update of Equation 5.34 can be substituted for the full replacement of the momentum in the standard HMC algorithm. This gives a generalized HMC algorithm in which an iteration consists of three steps:

1. Update the momentum variables using Equation 5.34. Let the new momentum be p'.
2. Propose a new state, (q^*, p^*), by applying L leapfrog steps with stepsize ε, starting at (q, p'), and then negating the momentum. Accept (q^*, p^*) with probability

$$\min\left[1, \exp\left(-U(q^*) + U(q) - K(p^*) + K(p')\right)\right].$$

   If (q^*, p^*) is accepted, let $(q'', p'') = (q^*, p^*)$; otherwise, let $(q'', p'') = (q, p')$.
3. Negate the momentum, so that the new state is $(q'', -p'')$.

The transitions in each of these steps—$(q, p) \to (q, p')$, $(q, p') \to (q'', p'')$, and $(q'', p'') \to (q'', -p'')$—leave the canonical distribution for (q, p) invariant. The entire update therefore also leaves the canonical distribution invariant. The three transitions also each satisfy detailed balance, but the sequential combination of the three does *not* satisfy detailed balance (except when $\alpha = 0$). This is crucial, since if the combination were reversible, it would still result in random-walk behavior when L is small.

Note that omitting step (3) above would result in a valid algorithm, but then, far from suppressing random walks, the method (with α close to one) would produce nearly back-and-forth motion, since the direction of motion would reverse with every trajectory accepted in step (2). With the reversal in step (3), motion continues in the same direction as long as the trajectories in step (2) are accepted, since the two negations of p will cancel. Motion reverses whenever a trajectory is rejected, so if random-walk behavior is to be suppressed, the rejection rate must be kept small.

If $\alpha = 0$, the above algorithm is the same as standard HMC, since step (1) will completely replace the momentum variables, step (2) is the same as for standard HMC, and step (3) will

have no effect, since the momentum will be immediately replaced anyway, in step (1) of the next iteration.

Since this algorithm can be seen as a generalization of standard HMC, with an additional α parameter, one might think it will offer an improvement, provided that α is tuned for best performance. However, Kennedy and Pendleton (2001) show that when the method is applied to high-dimensional multivariate Gaussian distributions only a small constant factor improvement is obtained, with no better scaling with dimensionality. Best performance is obtained using long trajectories (L large), and a value for α that is not very close to one (but not zero, so the optimum choice is not standard HMC). If L is small, the need to keep the rejection rate very low (by using a small ε), as needed to suppress random walks, makes the method less advantageous than standard HMC.

It is disappointing that only a small improvement is obtained with this generalization when sampling a multivariate Gaussian, due to limitations that likely apply to other distributions as well. However, the method may be more useful than one would think from this. For reasons discussed in Sections 5.4.3 and 5.4.5, we will often combine HMC updates with other MCMC updates (perhaps for variables not changed by HMC). There may then be a tradeoff between using long trajectories to make HMC more efficient, and using shorter trajectories so that the other MCMC updates can be done more often. If shorter-than-optimal trajectories are to be used for this reason, setting α greater than zero can reduce the random-walk behavior that would otherwise result.

Furthermore, rejection rates can be reduced using the "window" method described next. An analysis of partial momentum refreshment combined with the window method might find that using trajectories of moderate length in conjunction with a value for α greater than zero produces a more substantial improvement.

5.5.4 Acceptance Using Windows of States

Figure 5.3 (right plot) shows how the error in H varies along a typical trajectory computed with the leapfrog method. Rapid oscillations occur, here with a period of between 2 and 3 leapfrog steps, due to errors in simulating the motion in the most confined direction (or directions, for higher-dimensional distributions). When a long trajectory is used to propose a state for HMC, it is essentially random whether the trajectory ends at a state where the error in H is negative or close to zero, and hence will be accepted with probability close to one, or whether it happens to end at a state with a large positive error in H, and a correspondingly lower acceptance probability. If somehow we could smooth out these oscillations, we might obtain a high probability of acceptance for all trajectories.

I introduced a method for achieving this result that uses "windows" of states at the beginning and end of the trajectory (Neal, 1994). Here, I will present the method as an application of a general technique in which we probabilistically map to a state in a different space, perform a Markov chain transition in this new space, and then probabilistically map back to our original state space (Neal, 2006).

Our original state space consists of pairs, (q, p), of position and momentum variables. We will map to a sequence of W pairs, $[(q_0, p_0), \ldots, (q_{W-1}, p_{W-1})]$, in which each (q_i, p_i) for $i > 0$ is the result of applying one leapfrog step (with some fixed stepsize, ε) to (q_{i-1}, p_{i-1}). Note that even though a point in the new space seems to consist of W times as many numbers as a point in the original space, the real dimensionality of the new space is the same as the old, since the whole sequence of W pairs is determined by (q_0, p_0).

To probabilistically map from (q, p) to a sequence of pairs, $[(q_0, p_0), \ldots, (q_{W-1}, p_{W-1})]$, we select s uniformly from $\{0, \ldots, W-1\}$, and set (q_s, p_s) in the new state to our current state

(q,p). The other (q_i,p_i) pairs in the new state are obtained using leapfrog steps from (q_s,p_s), for $i>s$, or backwards leapfrog steps (i.e. done with stepsize $-\varepsilon$) for $i<s$. It is easy to see, using the fact that leapfrog steps preserve volume, that if our original state is distributed with probability density $P(q,p)$, then the probability density of obtaining the sequence $[(q_0,p_0),\ldots,(q_{W-1},p_{W-1})]$ by this procedure is

$$P\left([(q_0,p_0),\ldots,(q_{W-1},p_{W-1})]\right) = \frac{1}{W}\sum_{i=0}^{W-1} P(q_i,p_i), \tag{5.35}$$

since we can obtain this sequence from a (q,p) pair that matches any pair in the sequence, and the probability is $1/W$ that we will produce the sequence starting from each of these pairs (which happens only if the random selection of s puts the pair at the right place in the sequence).

Having mapped to a sequence of W pairs, we now perform a Metropolis update that keeps the sequence distribution defined by Equation 5.35 invariant, before mapping back to the original state space. To obtain a Metropolis proposal, we perform $L-W+1$ leapfrog steps (for some $L \geq W-1$), starting from (q_{W-1},p_{W-1}), producing pairs (q_W,p_W) to (q_L,p_L). We then propose the sequence $[(q_L,-p_L),\ldots,(q_{L-W+1},-p_{L-W+1})]$. We accept or reject this proposed sequence by the usual Metropolis criterion, with the acceptance probability being

$$\min\left[1,\ \frac{\sum_{i=L-W+1}^{L} P(q_i,p_i)}{\sum_{i=0}^{W-1} P(q_i,p_i)}\right], \tag{5.36}$$

with $P(q,p)\propto\exp(-H(q,p))$. (Note here that $H(q,p)=H(q,-p)$, and that starting from the proposed sequence would lead symmetrically to the original sequence being proposed.)

This Metropolis update leaves us with either the sequence $[(q_L,p_L),\ldots,(q_{L-W+1},p_{L-W+1})]$, called the "accept window," or the sequence $[(q_0,p_0),\ldots,(q_{W-1},p_{W-1})]$, called the "reject window." (Note that these windows will overlap if $L+1<2W$.) We label the pairs in the window chosen as $[(q_0^+,p_0^+),\ldots,(q_{W-1}^+,p_{W-1}^+)]$. We now produce a final state for the windowed HMC update by probabilistically mapping from this sequence to a single pair, choosing (q_e^+,p_e^+) with probability

$$\frac{P(q_e^+,p_e^+)}{\sum_{i=0}^{W-1} P(q_i^+,p_i^+)}.$$

If the sequence in the chosen window was distributed according to Equation 5.35, the pair (q_e^+,p_e^+) chosen will be distributed according to $P(q,p)\propto\exp(-H(q,p))$, as desired. To see this, let $(q_{e+n}^+,\ p_{e+n}^+)$ be the result of applying n leapfrog steps (backward ones if $n<0$) starting at $(q_e^+,\ p_e^+)$. The probability density that $(q_e^+,\ p_e^+)$ will result from mapping from a sequence to a single pair can then be written as follows, considering all sequences that can contain (q_e^+,p_e^+) and their probabilities:

$$\sum_{k=e-W+1}^{e}\left[\frac{1}{W}\sum_{i=k}^{k+W-1} P(q_i^+,p_i^+)\right]\frac{P(q_e^+,p_e^+)}{\sum_{i=k}^{k+W-1} P(q_i^+,p_i^+)} = P(q_e^+,p_e^+).$$

The entire procedure therefore leaves the correct distribution invariant.

When $W>1$, the potential problem with ergodicity discussed at the end of Section 5.3.2 does not arise, since there is a nonzero probability of moving to a state only one leapfrog step away, where q may differ arbitrarily from its value at the current state.

It might appear that the windowed HMC procedure requires saving all $2W$ states in the accept and reject windows, since any one of these states might become the new state when a state is selected from either the accept window or reject window. Actually, however, at most three states need to be saved—the start state, so that forward simulation can be resumed after the initial backward simulation, plus one state from the reject window and one state from the accept window, one of which will become the new state after one of these windows is chosen. As states in each window are produced in sequence, a decision is made whether the state just produced should replace the state presently saved for that window. Suppose that the sum of the probability densities of states seen so far is $s_i = p_1 + \cdots + p_i$. If the state just produced has probability density p_{i+1}, it replaces the previous state saved from this window with probability $p_{i+1}/(s_i + p_{i+1})$.

I showed (Neal, 1994) that, compared to standard HMC, using windows improves the performance of HMC by a factor of 2 or more, on multivariate Gaussian distributions in which the standard deviation in some directions is much larger than in other directions. This is because the acceptance probability in Equation 5.36 uses an average of probability densities over states in a window, smoothing out the oscillations in H from inexact simulation of the trajectory. Empirically, the advantage of the windowed method was found to increase with dimensionality. For high-dimensional distributions, the acceptance probability when using the optimal stepsize was approximately 0.85, larger than the theoretical value of 0.65 for HMC (see Section 5.4.4).

These results for multivariate Gaussian distributions were obtained with a window size, W, much less than the trajectory length, L. For less regular distributions, it may be advantageous to use a much larger window. When $W = L/2$, the acceptance test determines whether the new state is from the first half of the trajectory (which includes the current state) or the second half; the new state is then chosen from one half or the other with probabilities proportional to the probability densities of the states in that half. This choice of W guards against the last few states of the trajectory having low probability density (high H), as might happen if the trajectory had by then entered a region where the stepsize used was too big.

The windowed variant of HMC may make other variants of HMC more attractive. One such variant (Section 5.5.1) splits the Hamiltonian into many terms corresponding to subsets of the data, which tends to make errors in H higher (while saving computation). Errors in H have less effect when averaged over windows. As discussed in Section 5.5.3, very low rejection rates are desirable when using partial momentum refreshment. It is easier to obtain a low rejection probability using windows (i.e. a less drastic reduction in ϵ is needed), which makes partial momentum refreshment more attractive.

Qin and Liu (2001) introduced a variant on windowed HMC. In their version, L leapfrog steps are done from the start state, with the accept window consisting of the states after the last W of these steps. A state from the accept window is then selected with probabilities proportional to their probability densities. If the state selected is k states before the end, k backwards leapfrog steps are done from the start state, and the states found by these steps along with those up to $W - k - 1$ steps forward of the start state form the reject window. The state selected from the accept window then becomes the next state with probability given by the analog of Equation 5.36; otherwise the state remains the same.

Qin and Liu's procedure is quite similar to the original windowed HMC procedure. One disadvantage of Qin and Liu's procedure is that the state is unchanged when the accept window is rejected, whereas in the original procedure a state is selected from the reject window (which might be the current state, but often will not be). The only other difference is that the number of steps from the current state to an accepted state ranges from $L - W + 1$ to L (average $L - (W + 1)/2$) with Qin and Liu's procedure, versus from $L - 2W + 2$

to L (average $L - W + 1$) for the original windowed HMC procedure, while the number of leapfrog steps computed varies from L to $L + W - 1$ with Qin and Liu's procedure, and is fixed at L with the original procedure. These differences are slight if $W \ll L$. Qin and Lin claim that their procedure performs better than the original on high-dimensional multivariate Gaussian distributions, but their experiments are flawed.*

Qin and Liu (2001) also introduce the more useful idea of weighting the states in the accept and reject windows nonuniformly, which can be incorporated into the original procedure as well. When mapping from the current state to a sequence of W weighted states, the position of the current state is chosen with probabilities equal to the weights, and when computing the acceptance probability or choosing a state from the accept or reject window, the probability densities of states are multiplied by their weights. Qin and Liu use weights that favor states more distant from the current state, which could be useful by usually causing movement to a distant point, while allowing choice of a nearer point if the distant points have low probability density. Alternatively, if one sees a window as a way of smoothing the errors in H, symmetrical weights that implement a better "low pass filter" would make sense.

5.5.5 Using Approximations to Compute the Trajectory

The validity of HMC does not depend on using the correct Hamiltonian when simulating the trajectory. We can instead use some approximate Hamiltonian, as long as we simulate the dynamics based on it by a method that is reversible and volume-preserving. However, the exact Hamiltonian must be used when computing the probability of accepting the endpoint of the trajectory. There is no need to look for an approximation to the kinetic energy, when it is of a simple form such as Equation 5.13, but the potential energy is often much more complex and costly to compute—for instance, it may involve the sum of log likelihoods based on many data points, if the data cannot be summarized by a simple sufficient statistic. When using trajectories of many leapfrog steps, we can therefore save much computation time if a fast and accurate approximation to the potential energy is available, while still obtaining exact results (apart from the usual sampling variation inherent in MCMC).

Many ways of approximating the potential energy might be useful. For example, if its evaluation requires iterative numerical methods, fewer iterations might be done than are necessary to get a result accurate to machine precision. In a Bayesian statistical application, a less costly approximation to the unnormalized posterior density (whose log gives the potential energy) may be obtainable by simply looking at only a subset of the data. This may not be a good strategy in general, but I have found it useful for Gaussian process models (Neal, 1998; Rasmussen and Williams, 2006), for which computation time scales as the cube of the number of data points, so that even a small reduction in the number of points produces a useful speedup.

Rasmussen (2003) has proposed approximating the potential energy by modeling it as a Gaussian process, inferred from values of the potential energy at positions selected during an initial exploratory phase. This method assumes only a degree of smoothness of the potential energy function, and so could be widely applied. It is limited, however, by the cost of

* In their first comparison, their method computes an average of 55 leapfrog steps per iteration, but the original only computes 50 steps, a difference in computation time which if properly accounted for negates the slight advantage they see for their procedure. Their second comparison has a similar problem, and it is also clear from an examination of the results (in their Table I) that the sampling errors in their comparison are too large for any meaningful conclusions to be drawn.

Gaussian process inference, and so is most useful for problems of moderate dimensionality for which exact evaluation of the potential energy is very costly.

An interesting possibility, to my knowledge not yet explored, would be to express the exact potential energy as the sum of an approximate potential energy and the error in this approximation, and to then apply one of the splitting techniques described in Section 5.5.1—exploiting either the approximation's analytic tractability (e.g. for a Gaussian approximation, with quadratic potential energy), or its low computational cost, so that its dynamics can be accurately simulated at little cost using many small steps. This would reduce the number of evaluations of the gradient of the exact potential energy if the variation in the potential energy removed by the approximation term permits a large stepsize for the error term.

5.5.6 Short-Cut Trajectories: Adapting the Stepsize without Adaptation

One significant disadvantage of HMC is that, as discussed in Section 5.4.2, its performance depends critically on the settings of its tuning parameters—which consist of at least the leapfrog stepsize, ϵ, and number of leapfrog steps, L, with variations such as windowed HMC having additional tuning parameters as well. The optimal choice of trajectory length (ϵL) depends on the global extent of the distribution, so finding a good trajectory length likely requires examining a substantial number of HMC updates. In contrast, just a few leapfrog steps can reveal whether some choice of stepsize is good or bad, which leads to the possibility of trying to set the stepsize "adaptively" during an HMC run.

Recent work on adaptive MCMC methods is reviewed by Andrieu and Thoms (2008). As they explain, naively choosing a stepsize for each HMC update based on results of previous updates—for example, reducing the stepsize by 20% if the previous 10 trajectories were all rejected, and increasing it by 20% if less than two of the 10 previous trajectories were rejected—undermines proofs of correctness (in particular, the process is no longer a Markov chain), and will in general produce points from the wrong distribution. However, correct results can be obtained if the degree of adaptation declines over time. Adaptive methods of this sort could be used for HMC, in much the same way as for any other tunable MCMC method.

An alternative approach (Neal, 2005, 2007) is to perform MCMC updates with various values of the tuning parameters, set according to a schedule that is predetermined or chosen randomly without reference to the realized states, so that the usual proofs of MCMC convergence and error analysis apply, but to do this using MCMC updates that have been tweaked so that they require little computation time when the tuning parameters are not appropriate for the distribution. Most of the computation time will then be devoted to updates with appropriate values for the tuning parameters. Effectively, the tuning parameters are set adaptively from a computational point of view, but not from a mathematical point of view.

For example, trajectories that are simulated with a stepsize that is much too large can be rejected after only a few leapfrog steps, by rejecting whenever the change (either way) in the Hamiltonian due to a single step (or a short series of steps) is greater than some threshold—that is, we reject if $|H(q(t+\epsilon), p(t+\epsilon)) - H(q(t), p(t))|$ is greater than the threshold. If this happens early in the trajectory, little computation time will have been wasted on this unsuitable stepsize. Such early termination of trajectories is valid, since any MCMC update that satisfies detailed balance will still satisfy detailed balance if it is modified to eliminate transitions either way between certain pairs of states.

With this simple modification, we can randomly choose stepsizes from some distribution without wasting much time on those stepsizes that turn out to be much too large. However, if we set the threshold small enough to reject when the stepsize is only a little too large, we may terminate trajectories that would have been accepted, perhaps after a substantial amount of computation has already been done. Trying to terminate trajectories early when the stepsize is smaller than optimal carries a similar risk.

A less drastic alternative to terminating trajectories when the stepsize seems inappropriate is to instead *reverse* the trajectory. Suppose that we perform leapfrog steps in groups of k steps. Based on the changes in H over these k steps, we can test whether the stepsize is inappropriate—for example, the group may fail the test if the standard deviation of H over the $k+1$ states is greater than some upper threshold or less than some lower threshold (any criterion that would yield the same decision for the reversed sequence is valid). When a group of k leapfrog steps fails this test, the trajectory stays at the state where this group started, rather than moving k steps forward, and the momentum variables are negated. The trajectory will now exactly retrace states previously computed (and which therefore need not be recomputed), until the initial state is reached, at which point new states will again be computed. If another group of k steps fails the test, the trajectory will again reverse, after which the whole remainder of the trajectory will traverse states already computed, allowing its endpoint to be found immediately without further computation.

This scheme behaves the same as standard HMC if no group of k leapfrog steps fails the test. If there are two failures early in the trajectory, little computation time will have been wasted on this (most likely) inappropriate stepsize. Between these extremes, it is possible that one or two reversals will occur, but not early in the trajectory; the endpoint of the trajectory will then usually not be close to the initial state, so the nonnegligible computation performed will not be wasted (as it would be if the trajectory had been terminated).

Such short-cut schemes can be effective at finding good values for a small number of tuning parameters, for which good values will be picked reasonably often when drawing them randomly. It will not be feasible for setting a large number of tuning parameters, such as the entries in the "mass matrix" of Equation 5.5 when dimensionality is high, since even if two reversals happen early on, the cost of using inappropriate values of the tuning parameters will dominate when appropriate values are chosen only very rarely.

5.5.7 Tempering during a Trajectory

Standard HMC and the variations described so far have as much difficulty moving between modes that are separated by regions of low probability as other local MCMC methods, such as random-walk Metropolis and Gibbs sampling. Several general schemes have been devised for solving problems with such isolated modes that involve sampling from a series of distributions that are more diffuse than the distribution of interest. Such schemes include parallel tempering (Geyer, 1991; Earl and Deem, 2005), simulated tempering (Marinari and Parisi, 1992), tempered transitions (Neal, 1996b), and annealed importance sampling (Neal, 2001). Most commonly, these distributions are obtained by varying a "temperature" parameter, T, as in Equation 5.21, with $T = 1$ corresponding to the distribution of interest, and larger values of T giving more diffuse distributions. Any of these "tempering" methods could be used in conjunction with HMC. However, tempering-like behavior can also be incorporated directly into the trajectory used to propose a new state in the HMC procedure.

In the simplest version of such a "tempered trajectory" scheme (Neal, 1999, Section 6), each leapfrog step in the first half of the trajectory is combined with multiplication of the momentum variables by some factor α slightly greater than one, and each leapfrog step

in the second half of the trajectory is combined with division of the momentum by the same factor α. These multiplications and divisions can be done in various ways, as long as the result is reversible, and the divisions are paired exactly with multiplications. The most symmetrical scheme is to multiply the momentum by $\sqrt{\alpha}$ before the first half step for momentum (Equation 5.18) and after the second half step for momentum (Equation 5.20), for leapfrog steps in the first half of the trajectory, and correspondingly, to divide the momentum by $\sqrt{\alpha}$ before the first and after the second half steps for momentum in the second half of the trajectory. (If the trajectory has an odd number of leapfrog steps, for the middle leapfrog step of the trajectory, the momentum is multiplied by $\sqrt{\alpha}$ before the first half step for momentum, and divided by $\sqrt{\alpha}$ after the second half step for momentum.) Note that most of the multiplications and divisions by $\sqrt{\alpha}$ are preceded or followed by another such, and so can be combined into a single multiplication or division by α.

It is easy to see that the determinant of the Jacobian matrix for such a tempered trajectory is one, just as for standard HMC, so its endpoint can be used as a proposal without any need to include a Jacobian factor in the acceptance probability.

Multiplying the momentum by an α that is slightly greater than one increases the value of $H(q, p)$ slightly. If H initially had a value typical of the canonical distribution at $T = 1$, after this multiplication, H will be typical of a value of T that is slightly higher.* Initially, the change in $H(q, p) = K(p) + U(q)$ is due entirely to a change in $K(p)$ as p is made bigger, but subsequent dynamical steps will tend to distribute the increase in H between K and U, producing a more diffuse distribution for q than is seen when $T = 1$. After many such multiplications of p by α, values for q can be visited that are very unlikely in the distribution at $T = 1$, allowing movement between modes that are separated by low-probability regions. The divisions by α in the second half of the trajectory result in H returning to values that are typical for $T = 1$, but perhaps now in a different mode.

If α is too large, the probability of accepting the endpoint of a tempered trajectory will be small, since H at the endpoint will likely be much larger than H at the initial state. To see this, consider a trajectory consisting of only one leapfrog step. If $\epsilon = 0$, so that this step does nothing, the multiplication by $\sqrt{\alpha}$ before the first half step for momentum would be exactly canceled by the division by $\sqrt{\alpha}$ after the second half step for momentum, so H would be unchanged, and the trajectory would be accepted. Since we want something to happen, however, we will use a nonzero ϵ, which will on average result in the kinetic energy decreasing when the leapfrog step is done, as the increase in H from the multiplication by $\sqrt{\alpha}$ is redistributed from K alone to both K and U. The division of p by $\sqrt{\alpha}$ will now not cancel the multiplication by $\sqrt{\alpha}$—instead, on average, it will reduce H by less than the earlier increase. This tendency for H to be larger at the endpoint than at the initial state can be lessened by increasing the number of leapfrog steps, say by a factor of R, while reducing α to $\alpha^{1/R}$, which (roughly) maintains the effective temperature reached at the midpoint of the trajectory.

Figure 5.9 illustrates tempered trajectories used to sample from an equal mixture of two bivariate Gaussian distributions, with means of [0 0] and [10 10], and covariances of I and $2I$. Each trajectory consists of 200 leapfrog steps, done with $\epsilon = 0.3$, with tempering done as described above with $\alpha = 1.04$. The left plots show how H varies along the trajectories; the right plots show the position coordinates for the trajectories. The

* This assumes that the typical value of H is a continuous function of T, which may not be true for systems that have a "phase transition." Where there is a discontinuity (in practice, a near-discontinuity) in the expected value of H as a function of T, making small changes to H, as here, may be better than making small changes to T (which may imply big changes in the distribution).

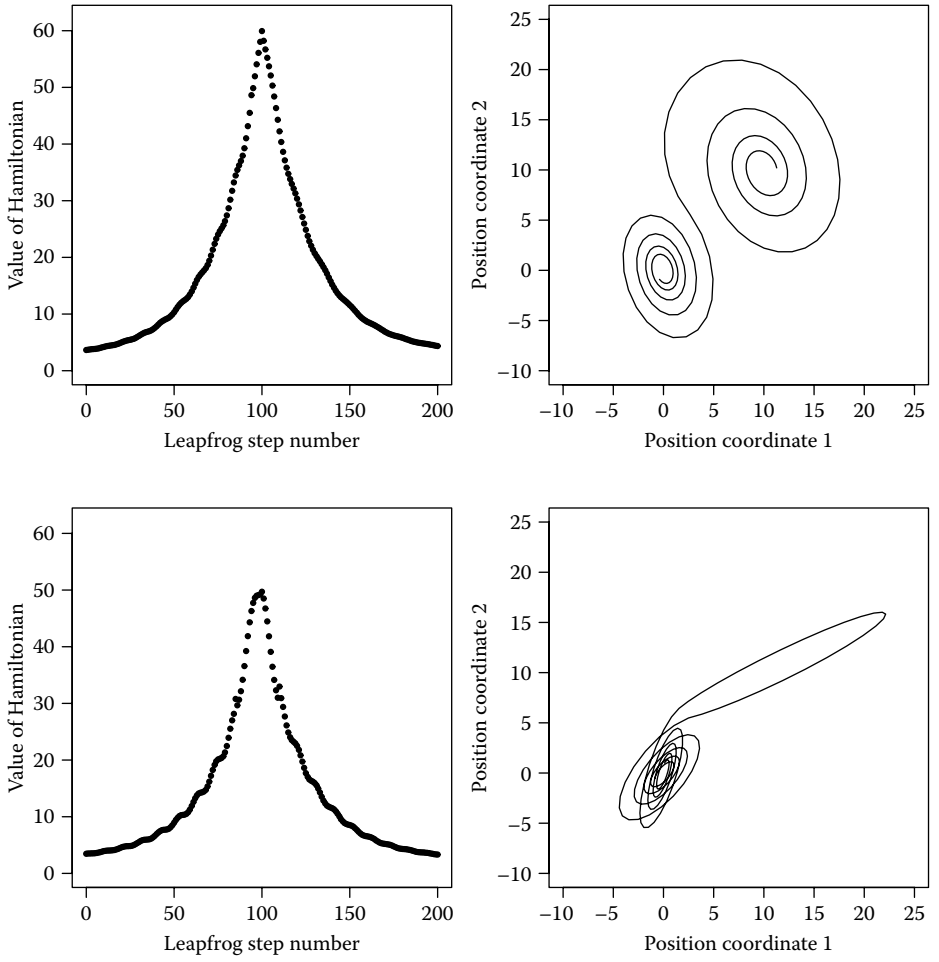

FIGURE 5.9
Illustration of tempered trajectories on a mixture of two Gaussians. The trajectory shown in the top plots moves between modes; the one shown in the bottom plots ends in the same mode.

top plots are for a trajectory starting at $q = [-0.4 \ \ -0.9]$ and $p = [0.7 \ \ -0.9]$, which has an endpoint in the other mode around [10 10]. The bottom plots are for a trajectory starting at $q = [0.1 \ 1.0]$ and $p = [0.5 \ 0.8]$, which ends in the same mode it begins in. The change in H for the top trajectory is 0.69, so it would be accepted with probability $\exp(-0.69) = 0.50$. The change in H for the bottom trajectory is -0.15, so it would be accepted with probability one.

By using such tempered trajectories, HMC is able to sample these two well-separated modes—11% of the trajectories move to the other mode and are accepted—whereas standard HMC does very poorly, being trapped for a very long time in one of the modes. The parameters for the tempered trajectories in Figure 5.9 were chosen to produce easily interpreted pictures, and are not optimal. More efficient sampling is obtained with a much smaller number of leapfrog steps, larger stepsize, and larger α—for example, $L = 20, \epsilon = 0.6$, and $\alpha = 1.5$ give a 6% probability of moving between modes.

A fundamental limitation of the tempering method described above is that (as for standard HMC) the endpoint of the tempered trajectory is unlikely to be accepted if the value for H there is much higher that for the initial state. This corresponds to the probability density at the endpoint being much lower than at the current state. Consequently, the method will not move well between two modes with equal total probability if one mode is high and narrow and the other low and broad, especially when the dimensionality is high. (Since acceptance is based on the joint density for q and p, there is some slack for moving to a point where the density for q alone is different, but not enough to eliminate this problem.) I have proposed (Neal, 1999) a modification that addresses this, in which the point moved to can come from anywhere along the tempered trajectory, not just the endpoint. Such a point must be selected based both on its value for H and the accumulated Jacobian factor for that point, which is easily calculated, since the determinant of the Jacobian matrix for a multiplication of p by α is simply α^d, where d is the dimensionality. This modified tempering procedure can not only move between modes of differing width, but also move back and forth between the tails and the central area of a heavy-tailed distribution.

More details on these variations on HMC can be found in the R implementations available from my web page, at www.cs.utoronto.ca/∼radford

Acknowledgment

This work was supported by the Natural Sciences and Engineering Research Council of Canada. The author holds a Canada Research Chair in Statistics and Machine Learning.

References

Alder, B. J. and Wainwright, T. E. 1959. Studies in molecular dynamics. I. General method. *Journal of Chemical Physics*, 31:459–466.

Andrieu, C. and Thoms, J. 2008. A tutorial on adaptive MCMC. *Statistics and Computing*, 18:343–373.

Arnold, V. I. 1989. *Mathematical Methods of Classical Mechanics*, 2nd edn. Springer, New York.

Bennett, C. H. 1975. Mass tensor molecular dynamics. *Journal of Computational Physics*, 19:267–279.

Caracciolo, S., Pelissetto, A., and Sokal, A. D. 1994. A general limitation on Monte Carlo algorithms of Metropolis type. *Physical Review Letters*, 72:179–182. Also available at http://arxiv.org/abs/hep-lat/9307021

Choo, K. 2000. Learning hyperparameters for neural network models using Hamiltonian dynamics. MSc thesis, Dept. of Computer Science, University of Toronto. Available at http://www.cs.toronto.edu/∼radford/ftp/kiam-thesis.pdf

Creutz, M. 1988. Global Monte Carlo algorithms for many-fermion systems. *Physical Review D*, 38:1228–1238.

Creutz, M. and Gocksch, A. 1989. Higher order hybrid Monte Carlo algorithms. *Physical Review Letters*, 63:9–12.

Duane, S., Kennedy, A. D., Pendleton, B. J., and Roweth, D. 1987. Hybrid Monte Carlo. *Physics Letters B*, 195:216–222.

Earl, D. J. and Deem, M. W. 2005. Parallel tempering: Theory, applications, and new perspectives. *Physical Chemistry Chemical Physics*, 7:3910–3916.

Frenkel, D. and Smit, B. 1996. *Understanding Molecular Simulation: From Algorithms to Applications*. Academic Press, San Diego, CA.

Geyer, C. J. 1991. Markov chain Monte Carlo maximum likelihood for dependent data. In E. M. Keramidas (ed.), *Computing Science and Statistics: Proceedings of the 23rd Symposium on the Interface*, pp. 156–163. American Statistical Association, New York.

Girolami, M., Calderhead, B., and Chin, S. A. 2009. Riemannian manifold Hamiltonian Monte Carlo. http://arxiv.org/abs/arxiv:0907.1100, 35 pp.

Grenander, U. and Miller, M. I. 1990. Representations of knowledge in complex systems. *Physics Letters B*, 242:437–443.

Gupta, S., Irbäck, A., Karsch, F., and Petersson, B. 1990. The acceptance probability in the hybrid Monte Carlo method. *Physics Letters B*, 242:437–443.

Hastings, W. K. 1970. Monte Carlo sampling methods using Markov chains and their applications. *Biometrika*, 57:97–109.

Horowitz, A. M. 1991. A generalized guided Monte Carlo algorithm. *Physics Letters B*, 268:247–252.

Ishwaran, H. 1999. Applications of hybrid Monte Carlo to generalized linear models: quasicomplete separation and neural networks. *Journal of Computational and Graphical Statistics*, 8:779–799.

Izagguirre, J. A. and Hampton, S. S. 2004. Shadow hybrid Monte Carlo: an efficient propagator in phase space of macromolecules. *Journal of Computational Physics*, 200:581–604.

Kennedy, A. D. 1990. The theory of hybrid stochastic algorithms. In P. H. Damgaard, H. Hüffel, and A. Rosenblum (eds), *Probabilistic Methods in Quantum Field Theory and Quantum Gravity*, pp. 209–223. Plenum Press, New York.

Kennedy, A. D. and Pendleton, B. 1991. Acceptances and autocorrelations in hybrid Monte Carlo. *Nuclear Physics B (Proc. Suppl.)*, 20:118–121.

Kennedy, A. D. and Pendleton, B. 2001. Cost of the generalized hybrid Monte Carlo algorithm for free field theory. *Nuclear Physics B*, 607:456–510. Also available at http://arxiv.org/abs/hep-lat/0008020

Leimkuhler, B. and Reich, S. 2004. *Simulating Hamiltonian Dynamics*. Cambridge University Press, Cambridge.

Liu, J. S. 2001. *Monte Carlo Strategies in Scientific Computing*. Springer, New York.

Mackenzie, P. B. 1989. An improved hybrid Monte Carlo method. *Physics Letters B*, 226:369–371.

Marinari, E. and Parisi, G. 1992. Simulated tempering: A new Monte Carlo scheme. *Europhysics Letters*, 19:451–458.

McLachlan, R. I. and Atela, P. 1992. The accuracy of symplectic integrators. *Nonlinearity*, 5: 541–562.

Metropolis, N., Rosenbluth, A. W., Rosenbluth, M. N., Teller, A. H., and Teller, E. 1953. Equation of state calculations by fast computing machines. *Journal of Chemical Physics*, 21:1087–1092.

Neal, R. M. 1993. Probabilistic inference using Markov chain Monte Carlo methods. Technical Report CRG-TR-93-1, Dept. of Computer Science, University of Toronto.

Neal, R. M. 1994. An improved acceptance procedure for the hybrid Monte Carlo algorithm. *Journal of Computational Physics*, 111:194–203.

Neal, R. M. 1996a. *Bayesian Learning for Neural Networks*, Lecture Notes in Statistics, Vol. 118. Springer, New York.

Neal, R. M. 1996b. Sampling from multimodal distributions using tempered transitions. *Statistics and Computing*, 6:353–356.

Neal, R. M. 1998. Regression and classification using Gaussian process priors (with discussion). In J. M. Bernardo, J. O. Berger, A. P. Dawid, and A. F. M. Smith (eds.), *Bayesian Statistics 6*, pp. 475–501. Oxford University Press, Oxford.

Neal, R. M. 1999. Markov chain sampling using Hamiltonian dynamics. Talk at the Joint Statistical Meetings, Baltimore, MD, August. Slides are available at http://www.cs.utoronto.ca/∼radford/ftp/jsm99.pdf

Neal, R. M. 2001. Annealed importance sampling. *Statistics and Computing*, 11:125–139.

Neal, R. M. 2005. The short-cut Metropolis method. Technical Report No. 0506, Department of Statistics, University of Toronto, 28 pp. Available at http://arxiv.org/abs/math.ST/0508060

Neal, R. M. 2006. Constructing efficient MCMC methods using temporary mapping and caching. Talk at Columbia University, Dept. of Statistics, December 11. Slides are available at http://www.cs.utoronto.ca/∼radford/ftp/cache-map.pdf

Neal, R. M. 2007. Short-cut MCMC: An alternative to adaptation. Talk at the Third Workshop on Monte Carlo Methods, Harvard, May. Slides are available at http://www.cs.utoronto.ca/~radford/ftp/short-mcmc-talk.pdf

Qin, Z. S. and Liu, J. S. (2001). Multipoint Metropolis method with application to hybrid Monte Carlo. *Journal of Computational Physics*, 172:827–840.

Rasmussen, C. E. 2003. Gaussian processes to speed up hybrid Monte Carlo for expensive Bayesian integrals. In J. M. Bernardo, M. J. Bayarri, J. O. Berger, A. P. Dawid, D. Heckerman, A. F. M. Smith, and M. West, (eds.), *Bayesian Statistics 7. Proceedings of the Seventh Valencia International Meeting*, pp. 651–659. Oxford University Press, Oxford.

Rasmussen, C. E. and Williams, C. K. I. 2006. *Gaussian Processes for Machine Learning*. MIT Press, Cambridge, MA.

Roberts, G. O., Gelman, A., and Gilks, W. R. 1997. Weak convergence and optimal scaling of random walk Metropolis algorithms. *Annals of Applied Probability*, 7:110–120.

Roberts, G. O. and Rosenthal, J. S. 1998. Optimal scaling of discrete approximations to Langevin diffusions. *Journal of the Royal Statistical Society*, *Series B*, 60:255–268.

Roberts, G. O. and Tweedie, R. L. 1996. Exponential convergence of Langevin distributions and their discrete approximations. *Bernoulli*, 2:341–363.

Rossky, P. J., Doll, J. D., and Friedman, H. L. 1978. Brownian dynamics as smart Monte Carlo simulation. *Journal of Chemical Physics*, 69:4628–4633.

Ruján, P. 1997. Playing billiards in version space. *Neural Computation*, 9:99–122.

Schmidt, M. N. 2009. Function factorization using warped Gaussian processes. In *Proceedings of the Twenty-Sixth International Conference on Machine Learning*. ACM, New York.

Sexton, J. C. and Weingarten, D. H. 1992. Hamiltonian evolution for the hybrid Monte Carlo method. *Nuclear Physics B*, 380:665–677.